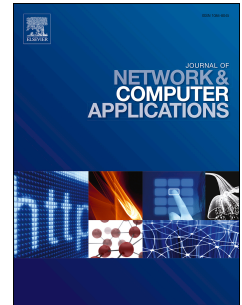# Accepted Manuscript

Device-free human localization and tracking with UHF passive RFID tags: A data-driven approach

Wenjie Ruan, Quan Z. Sheng, Lina Yao, Xue Li, Nickolas J.G. Falkner, Lei Yang

Please cite this article as: Ruan, W., Sheng, Q.Z., Yao, L., Li, X., Falkner, N.J.G., Yang, L., Device-free human localization and tracking with UHF passive RFID tags: A data-driven approach, *Journal of Network and Computer Applications* (2018), doi: 10.1016/j.jnca.2017.12.010.

Device-free Human Localization and Tracking with UHF Passive RFID Tags: A Data-driven Approach

Wenjie Ruan[a], Quan Z. Sheng[b], Lina Yao[c], Xue Li[d], Nickolas J.G. Falkner[a], Lei Yang[e]

[a]*Department of Computer Science, University of Oxford, Oxford, OX1 3QD, United Kingdom*
[b]*Department of Computing, Macquarie University, Sydney, NSW 2109, Australia*
[c]*School of Computer Science and Engineering, The University of New South Wales, Sydney, NSW 2052, Australia*
[d]*School of Information Technology and Electrical Engineering, The University of Queensland, Brisbane, Queensland 4072, Australia*
[e]*Department of Computing, The Hong Kong Polytechnic University, Kowloon, Hong Kong*

Abstract

Localizing and tracking human movement in a *device-free and passive* manner is promising in two aspects: *i)* it neither requires users to wear any sensors or devices, *ii)* nor it needs them to consciously cooperate during the localization. Such indoor localization technique underpins many real-world applications such as shopping navigation, intruder detection, surveillance care of seniors *etc.* However, current passive localization techniques either need expensive/sophisticated hardware such as ultra-wideband radar or infrared sensors, or have an issue of invasion of privacy such as camera-based techniques, or need regular maintenance such as the replacement of batteries. In this paper, we build a novel *data-driven* localization and tracking system upon a set of commercial ultra-high frequency passive radio-frequency identification tags in an indoor environment. Specifically, we formulate human localization problem as finding a location with the maximum posterior probability given the observed received signal strength indicator from passive radio-frequency identification tags. In this regard, we design a series of localization schemes to capture the posterior probability by taking the advance of supervised-learning models including Gaussian Mixture Model, k Nearest Neighbor and Kernel-based Learning. For tracking a moving target, we mathematically model the task as searching a location sequence with the most likelihood, in which we first augment the probabilistic estimation learned in localization to construct the Emission Matrix and propose two human mobility models to approximate the Transmission Matrix in the Hidden Markov Model. The proposed tracking model is able to transfer the pattern learned in localization into tracking but also reduce the location-state candidates at each transmission iteration, which increases both the computation efficiency and tracking accuracy. The extensive experiments in two real-world scenarios reveal that our approach can achieve up to 94% localization accuracy and an average $0.64m$ tracking error, outperforming other state-of-the-art radio-frequency identification based indoor localization systems.

Keywords: RFID, Hidden Markov Model, Gaussian Mixture Model, Device-free, Indoor Localization, Tracking

1. Introduction

With the explosively increasing aging population, intelligent space that can better support the independent living of the elderly has been attracting the increasing attention both from industry and academia. One of the key preconditions for such a smart environment lies on an accurate and timely detection of users' locations and daily routines [1, 2], especially for an *indoor environment* that GPS (Global Position System) cannot handle [3]. To tackle this challenge, a wide range of indoor localization and tracking systems have been proposed for the last two decades, including but not limited to LANDMARC [4], WILL [5], Tagoram [6] and BackPos [7]. However most of the approaches are wearable-device based technique that inevitably requires the user to actively carry one or more devices such as various types of sensors, smart-phones, RFID tags/readers or other Radio Frequency (RF) transceivers, thus raising many in-

herent impractical issues in reality [8]. For example, the attached sensors/tags may be damaged or lost. It is also obstructive and inconvenient for the user to wear devices all the time[1], especially considering that many electronic devices have a moderate size or weight.

For this end, *device-free* (also called *unobtrusive*) passive indoor localization has gained more attention lately and many promising approaches have been proposed [9, 10, 11, 12]. One popular device-free human tracking technique is built upon the recent advance of computer vision, which develops various models to capture human movement from images or videos by using RGB cameras [13, 14], or infrared sensors [15] or depth cameras (*e.g.,* Kinect) [16]. However computer vision based approaches require the tracked user within the line-of-sight[2] (LOS) of a camera, and usually fail to work in a dimmed environment [13]. Moreover, vision-based technique can also be

---

Email addresses: wenjie.ruan@cs.ox.ac.uk (Wenjie Ruan), michael.sheng@mq.edu.au (Quan Z. Sheng)

[1]Deloitte Mobile Consumer Survey 2016: `www2.deloitte.com/au/en/pages/technology-media-and-telecommunications/articles/mobile-consumer-survey-2016.html`

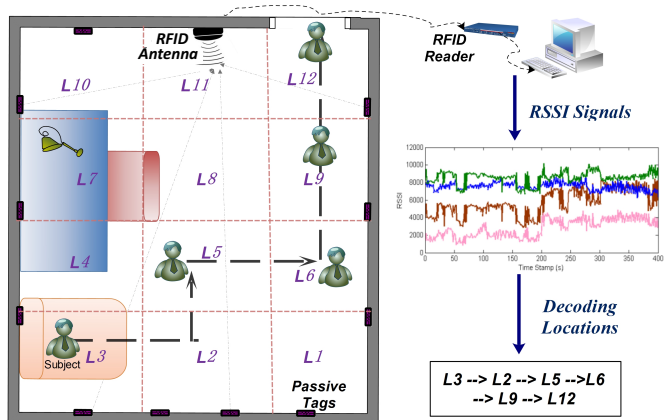[2]There are no barriers or blocks between the subject and camera.

Figure 1: The general idea of the proposed DfP localization and tracking system

considered to be privacy invasive [1]. Another DfP localization technique is to intensively exploit the radio-frequency signal, *e.g.,* localizing the target by analyzing the Received Signal Strength (RSS) variations [17, 18, 2] or Channel State Information (CSI) [19, 20] in WIFI, or tracking the user through a wall by decoding the radiowaves reflected of human movement [21]. Though promising, these systems often require specialized RF signals such as Frequency-Modulated Continuous Wave (FMCW) or build upon costly special-purpose devices such as USRP (universal software radio peripheral), or need to modify the low-level firmware such as abstracting CSI signals. Most importantly, they all require regular maintenance such as battery replacement, thus hindering their practical deployment in the real world [1, 8]. In this regard, device-free tracking systems built on COTS (commercial off-the-shelf) passive RFID tags are more promising in terms of deployment convenience (commercialized product without any hardware or firmware modification), maintenance effort (no batteries needed and purely harvesting the in-air backscattered energy) and cost efficiency (≈5 cents each, still dropping quickly) [22, 23, 24, 25]. As a result, in this paper, we design a DfP system that can unobtrusively localize, track a subject to high accuracy based on *pure* passive RFID tags.

However, applying this high-level idea into a practical indoor localization and tracking system is a non-trivial and challenging task. One key challenge lies on the fact that, in a practical residential environment, RSSI signal is quite complex and unstable because of the multipath effect, power source fluctuation and ambient noise disturbance. Unlike the theoretical analysis, the practical RSSI signal however does not strictly decrease along with tag-reader distance and exhibits significant nonlinearity, and it may be further corrupted when introducing human motion. Another challenging issue is how to model the localization and tracking problem from a data-driven point of view. Currently, most of existing RFID-based systems are built upon the signal propagation model or backscatter communication mechanism, thus there is no off-the-shelf learning-based localization model for us to use. Moreover, to reduce the learning burden, we intend to transfer the pattern learned in localizing a stationary person into tracking a moving subject. Thus how to

effectively bridge the gap between localization and tracking under a feasible mathematical framework also deserves a careful resolution.

To tackle the aforementioned challenges, we first need to enable the RSSI signal from passive tags to monitor the whole surveillance area in an efficient and unobtrusive manner. Thus we deploy a set of passive RFID tags and a reader (with antennas) to form a RSS field that can cover the whole monitored area. Fig. 1 outlines the general hardware deployment in our system. Specially, unlike other RFID-based systems that place the tags on the ground [11, 10], we attach the passive tags and antennas on the wall to *i)* make the RSSI signal face fewer obstacles and *ii)* not obstruct to user's routine activities, especially in a residential environment. Based upon our RFID infrastructure, some distinguishable patterns can be clearly observed in RSSI signals when a user appears in different locations of a room. In summary, our RFID-based system is intuitively based on two experimental observations:

Observation 1. *The RSSI vector illustrates differentiable changes when a user appears in an RSS-monitored area comparing to a non-subject scenario.*

Observation 2. *The RSSI vector reveals distinguishable fluctuation patterns when a user presents in different locations within an RSS-monitored zone.*

The above two observations substantially illustrate that distributions of a RSSI vector[3] are directly relevant with a user's indoor positions, and those distributions are differentiable for different locations. Motivated by these two experimental phenomena, we thus seek to decode human locations and motions by using data-driven approaches. Specifically, to localize a stationary person, we mathematically formulate it as a classification problem, in which we first collect the RSSIs and associated location labels to train a location classifier that is then utilized to predict user's actual location according to the observed RSSI vector (see details in Sec. 4). For tracking a moving user, we first augment the traditional kNN with probabilistic information to quantify the likelihood of locations based on observed RSSIs, which then is utilized to construct the Emission Matrix in HMM. Furthermore, we calculate the Transmission Matrix by introducing two location transition strategies - *Constraint-Less Transition* (CLT) and *Constraint Transition* (CT). The latter transition strategy allows our system to largely narrow down the candidate locations at each state transmission in HMM, which turns out to only not minimize the computation overhead but also increase the tracking accuracy (see details in Sec. 5). At last, we use Viterbi Search to find the most likely path of the subject. We call this kNN-HMM. In a nutshell, we summarize the main contributions in the paper as below:

• We design a device-free indoor localization and tracking system that utilizes COTS passive RFID tags and bears some

---

[3]For example, in Fig. 1, we can formulate the RSSIs of all tags at a certain time-stamp as a vector containing 11 readings.
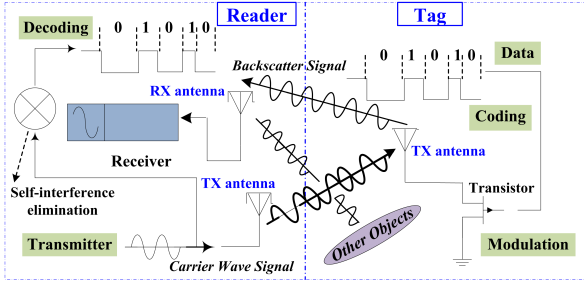
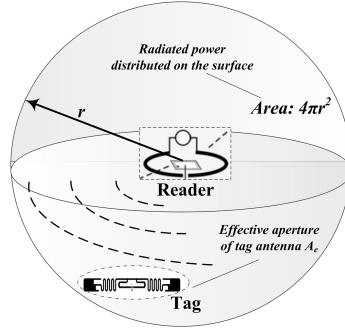Figure 2: Backscatter communication mechanism

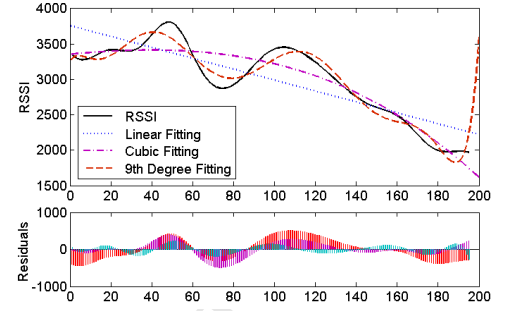Figure 3: Path loss illustration

Figure 4: RSSI variation with distance

promising characteristics in terms of hardware cost, deployment scalability and maintenance burden. To the best of our knowledge, the designed system, purely built upon passive RFID tags, is one of the device-free works that can not only localize a *stationary* user but also track a *moving* one with a high accuracy in a real-world *residential* environment.

- We introduce a kNN based HMM method to tracking a motion person by learning the underlying impacts of a non-moving human body to RSSIs for different locations, which to some extent bridges the gap of localization to tracking from a data-driven point of view.

- We conduct extensive in-suit experiments in a real-world residential house where participants unconstrainedly simulate a series of practical daily living routines. The experimental results demonstrate that our system achieves over 94% localization accuracy and $0.64m$ mean tracking error while largely reducing the training overhead to 2 minutes for a $17m^2$ bedroom.

We organize the remaining paper as follows. Sec. 2 illustrates our preliminary analysis and experiential observations. We then mathematically model our target localization and tracking problems in Sec. 3. In the next, we highlight the proposed solutions in Sec. 4 and Sec. 5. The experimental results are presented in Sec. 6. Then we overview related work in Sec. 7. Finally, some discussions and concluding remarks are offered in Sec. 8.

2. Preliminary

In this section, we will theoretically analyze the RFID backscatter radio signal and then verify our system's capability to reach device-free localization and tracking.

2.1. Backscatter Radio Communication

RFID tags are widely applied in many industries, for example, an RFID tag attached to an automobile during production can be utilized to monitored its progress in the assembling, RFID-tagged containers can be tracked during the transportation [26, 27]. Unlike active RFID tags that are powered by batteries, passive RFID systems however communicate through the backscatter radio links due to that passive tags (no batteries powered) can only passively collect energy from the in-air

backscattered radio signal. Fig. 2 illustrates a conceptual diagram of the radio wave propagation between an RFID reader and a passive tag. In details, the current flow on a reader-antenna induces to a voltage on the tag-antenna (integrated in the circuit), further producing a radiation signal. The radiated wave then makes its way back to the reader-antenna, inducing a voltage, thus producing a signal that can be detected: a backscattered signal. Specially, the tag transmits "1" bit by changing the impedance on their antennas to reflect the readers signal and a "0" bit by remaining in their initial silence state [28], called ON-OFF keying. A typical UHF reader works in the frequency band from 860 MHz~950 MHz (*e.g.,* $902 \sim 928MHz$ ISM band in US). Today's commercialized RFID readers have an interrogation distance of about 10 $meter$, which is enough for a residential environment. More importantly, the electromagnetic field produced by RFID readers under no circumstance will harm the human body[4].

2.2. Received Signal Strength Indicator (RSSI)

RSSI measures the power of received radio signal between the tag-antenna and reader-antenna [28]. Shown as Fig. 3, *Path Loss* represents the power difference of signals from the receiving antenna and the transmitting antenna. We assume the radiated power as being uniformly distributed over a spherical surface at given distance r from the reader-antenna. Then, only part of this power is received by a tag-antenna, represented as $P_{RX} = P_{TX}A_e/4\pi r^2$. Since the effective aperture of an antenna around a half-wavelength long corresponds to a square round a half-wavelength on a side, the path loss for the isotropic link can be estimated by $A_e = G\lambda^2/4\pi$ where G denotes the gain of an antenna. Thus we can calculate *Friis Equation* of the power from the transmission-antenna TX to the receiver-antenna RX [28].

$$P_{RX} = P_{TX}G_{TX}\frac{A_{e,RX}}{4\pi r^2} = P_{TX}G_{TX}G_{RX}(\frac{\lambda}{4\pi r})^2 \quad (1)$$

Then, we can mathematically model the backscatter signal prorogation as:

$$\begin{aligned} P_{RX,reader} &= P_{TX,tag}G_{tag}G_{reader}(\lambda/4\pi r)^2 \\ &= P_{TX,reader}T_bG_{tag}^2G_{reader}^2(\lambda/4\pi r)^4 \end{aligned} \quad (2)$$

---

[4]Is RFID Dangerous? www.inria.fr/en/centre/lille/news/is-rfid-dangerous

3

where G_{tag} denotes the gain of the tag-antenna and T_b represents the loss of backscatter transmission. Thus, under an assumption that a wave directly leaves the antenna and strikes the tag (*i.e.,* interacting with no other objects), Eqn. 2 theoretically demonstrates that the power received by the reader-antenna is inversely proportional to the fourth power of the reader-tag distance. Thereby, for a cleared or open space, RSSIs is capable of being a promising location indicator. However, our system targets to enable a device-free tracking in a cluttered environment. As Fig. 4 shows, the RSSI strength shows a uncertain nonlinearity with the distance in a residential room, which cannot be expressed by a *cubic* or even a *9th-degree polynomial* model. So how to model the RSSI-location relation for our application scenario is very challenging. Instead of developing delicate signal propagation models[5], this paper intends to seek the answer from a data-driven point of view, *i.e.,* accurately learning the quantifying relation between the user's location and the interference of human body to RSSIs from the collected RSSI observations. We will elaborate the details in Sec. 4.

2.3. Intuitions Verification

In this section, we conduct several pilot experiments to demonstrate the localization potentials of our system. We first build a testbed consisted of one RFID reader and 4 UHF passive tags. The monitored area is divided into 9 virtual grids ($0.6m \times 0.6m$ each), representing 9 different zones $L_1, L_2, ..., L_9$. We want to verify whether the RSSI patterns reveal distinguishable differences when a user appears in different grids. Fig. 5 snapshots our pilot experimental results. At first, there is no user in the monitored area, then a person stands in L_5 and L_9. We observe that the measured four RSSI signals obviously vary due to the presence of a subject, so we can clearly discriminate whether there is a subject in the RSS field or not. We also find that the RSSI signal shows different fluctuation patterns when the subject stands in L_5 and L_9. We further cluster the RSSI data generated from these three scenarios (*i.e.,* no subject, L_5 and L_9) into a four-dimension space (illustrated by two 3-D scattering figures). It clearly shows the data clustering in three different subareas (revealing the number of locations the subject ever appeared) even without overlapping (can be learned to infer the exact human locations). In summary, the preliminary experiments reveal the intuitions and feasibility behind our system for solving the device-free localization. However, in a residential environment, how to accurately decode the accurate locations is still a non-trivial problem considering the complicated multi-path effect and the unstable backscattered RSSI propagation properties. We will elaborate it in Sec. 5.

3. Problem Formulation

As aforementioned, we intend to pinpoint the subject's locations and estimate its continuous trajectory based on the received RSSIs from a set of RFID tags. Thus we can formally
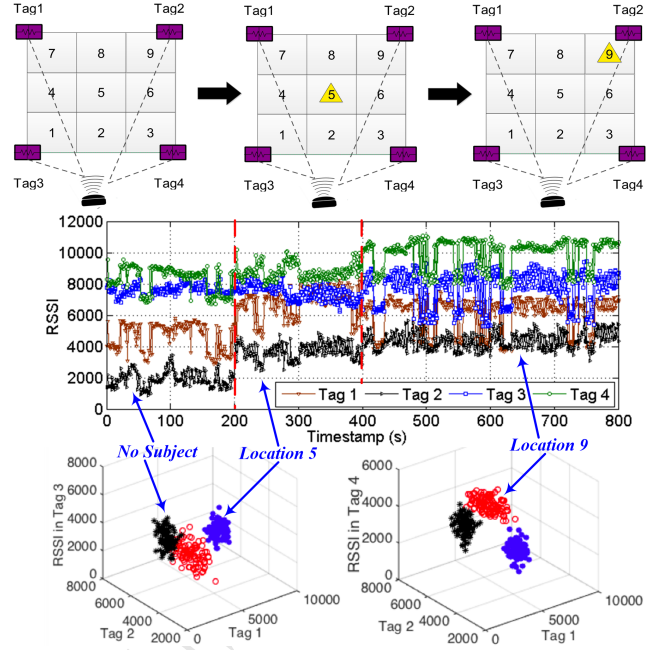

Figure 5: The RSSI readings cluster in differentiable spaces when a person appears in different locations

define the two targeted problems - *localization* and *tracking* - in this paper as follows.

Problem 1 (Localization). *In a monitored area covered by one or more RSS fields, can we accurately pinpoint the current location of a stationary user given a set of RSSI vectors?*

Problem 2 (Tracking). *In a monitored area covered by one or more RSS fields, can we continuously estimate the motion trajectory of a moving user with a moderate speed (less than $1m/s$) given a sequence of time-tagged RSSI vectors?*

Fig. 6 illustrates the pipeline of our solutions for the two problems. From a data-driven point of view, *Problem 1 - Localization* can substantially be reformulated as a location classification problem, in which we aim to accurately quantify the RSSI distributions for different geographical locations within the monitored area. Specifically, assuming that D anchoring passive tags are deployed in a surveillance area which is divided into G small grids, we then can represent the locations as $\mathbf{l} = \{l_0, l_1, ..., l_G\}$ where l_i means the subject appears in location i and l_0 indicates the area is empty. In the next, we collect profiling dataset in the following two steps: *i)* we record the RSSI readings of all anchoring tags when no human body in the monitored area; and *ii)* then a user appears in location $l_i, (i = 1, 2, ..., G)$ and collect the corresponding RSSI values. Then we build a training dataset $\mathcal{H} = \{\mathbf{S}_0, \mathbf{S}_1, ..., \mathbf{S}_G\}$, where $\mathbf{S}_i \in \mathbb{R}^{N \times D}$, N is the sample number in each grid. This dataset contains the latent information regarding how a human body influences the RSSIs' distribution for each location plus an empty environment. We further can quantify the underlying *RSSI-Location* relationship by training a classification model using $\mathcal{H}$. Finally, we construct a $(G + 1)$-location classifier. During
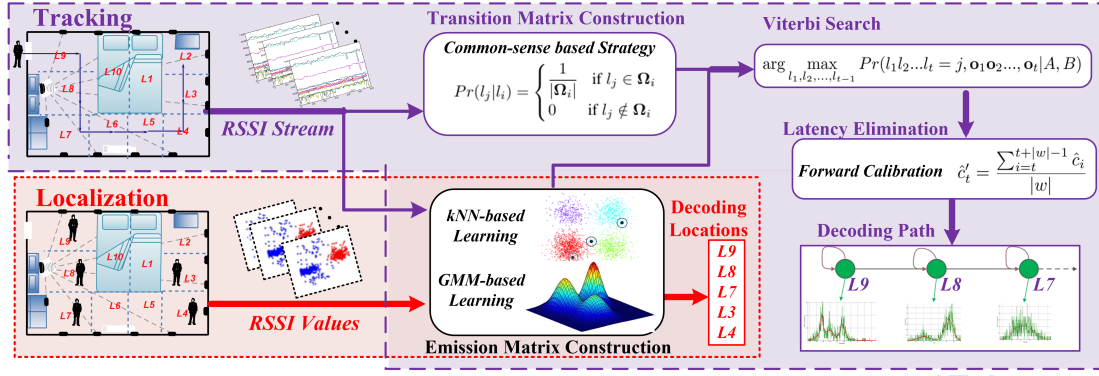
---

[5]This kind of models is also highly related to the furniture and room layout, thereby it is hard to design a physical localization model with satisfying robustness and accuracy.

Figure 6: The system architecture

localization phase, a user randomly stands on any locations in the surveillance area, and the corresponding RSSI vectors are collected and fed into the location classier. Then it will output location labels that associate with the subject's actual locations.

Assuming that the collected RSSI observation dataset is represented by $\mathcal{R} = \{\mathbf{r}_1, \mathbf{r}_2, ..., \mathbf{r}_T\}$, Problem 1 is mathematically formulated as estimating the optimal posterior probability distribution $p(l_j|\mathbf{r}_i)$ given a RSSI observation sequence.

$$j^* = \arg \max_j Pr(l_j|\mathbf{r}_i) \qquad (3)$$

In Sec. 4, we will give the technical details regarding how to solve the above optimization problem.

Similarly, for *Problem 2-Tracking*, we can model it as estimating the joint probability distribution upon the RSSI observation sequence $R_{1:T}$ and the location labels $l_{1:T}$ where its location state at time-stamp t is denoted by l_t. We can further simplify the model by assuming that the dynamic motion is a Markov process which only depends on previous location state, represented by model $Pr(l_j|l_{j-1})$. In this end, we need to solve the following mathematical problem:

$$Pr(\mathbf{r}_{1:T}, l_{1:T}) = Pr(l_1)Pr(\mathbf{r}_1|l_1)\prod_{t=2}^{T} Pr(\mathbf{r}_t|l_t)Pr(l_t|l_{t-1}) \qquad (4)$$

to estimate the expected location states $l_{1:T}$ with the maximum probability. We also need to train a marginal posterior $Pr(\mathbf{s}_i|l_{1:j})$ to estimate the expected value of l_j given observed RSSI readings. We will introduce the technical details in Sec. 5.

4. Localizing Stationary Subject

This section will introduce three location classifiers, *i.e., Multivariate Gaussian Mixture Model*, k *Nearest Neighbor*, and *Kernel-based Localization* for solving Problem 1 - estimating user's location given a set of RSSI vectors.

4.1. Gaussian Mixture Model based Localization

According to our previous analysis, the key part of localization is to model $Pr(l_j|\mathbf{r}_i)$, the probability distribution of locations given RSSI observation. This task is difficult since it needs to quantify the distribution of an underlying variable.

However, the reversed distribution $Pr(\mathbf{r}_j|l_i)$ can be easily learned by observing how RSSIs distribute given the location of a user. Based on the *Bayes Theorem*, we thereby decompose the distribution $Pr(l|\mathbf{r})$ as follows[6] :

$$Pr(l|\mathbf{r}) = \frac{Pr(\mathbf{r}|l)Pr(l)}{Pr(\mathbf{r})} \propto Pr(\mathbf{r}|l) \cdot Pr(l) \qquad (5)$$

where we assume $Pr(l) \sim 1/G$, denoting an uniform distribution at location l. The assumption lies on the fact that a user may appear in any locations with an equal probability. In the next, we need to find an appropriate model that quantifies $Pr(\mathbf{r}|l)$ distribution. Then we can transfer Eqn. 3 as the following optimization problem.

$$l^* = \arg \max_{l \in \mathbf{l}} Pr(\mathbf{r}|l) \cdot Pr(l) \qquad (6)$$
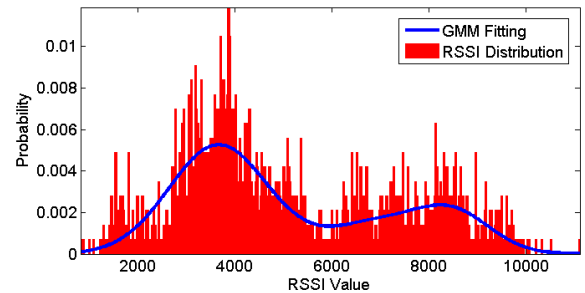
Figure 7: RSSI distribution pattern and fitted by GMM

In our pilot experiment, we observe that RSSIs display a certain clustering pattern in the high-dimension space. When we take a close look at each cluster, it actually shows a multimodal distribution that follows a Gaussian Mixture Model, as shown in Fig. 7. This RSSI distribution phenomenon in fact can be explained by the multi-path effect [28, 29]. Normally, several paths for the backscattered signal exist during the propagation from a tag to a reader. Among all the paths, the reader prefers to resolve the strongest signal path. When a human

---
[6] For simplicity, we drop i and j in the equation.

body blocks some propagation paths (*i.e.,* a subject appears in the RSS field), it will cause the propagation to jump among the multiple paths and lead to the strength migrating from one level to another. As a result, the signal strength exhibits multi-modal characteristics - the distribution is likely composed of multiple Gaussian models. Thus, we can utilize a GMM to capture the probability distribution when a user appears in each grid. Specifically, we propose a Gaussian Mixture Model with m Gaussian components as follows:

$$
\begin{aligned}
f_l(x) = Pr(x|l) &= \sum_{m=1}^{M} q_{l,m} \mathcal{N}(x|\mu_{l,m}, \boldsymbol{\Sigma}_{l,m}) \\
&= \sum_{m=1}^{M} \frac{q_{l,m}}{\sqrt{(2\pi)^{\mathcal{D}} |\boldsymbol{\Sigma}_{l,m}|}} \exp(-\frac{1}{2}(x - \mu_{l,m})^T \boldsymbol{\Sigma}_{l,m}^{-1}(x - \mu_{l,m}))
\end{aligned}
$$
(7)

where $\boldsymbol{\Phi}_l = \{q_{l,m}, \mu_{l,m}, \Sigma_{l,m}\}$ represents the model parameter set for location l, in which $q_{l,m}$ means the weighted factor for the mth mixture component, $\mu_{l,m}$ and $\boldsymbol{\Sigma}_{l,m}$ denote the mean and covariance in the mth Gaussian component. Furthermore, by using the maximum likelihood estimation, the optimal model parameters $\hat{\boldsymbol{\Phi}}_l$ can be learned through

$$
\hat{\boldsymbol{\Phi}}_l = \arg\max_{\boldsymbol{\Phi}_l} Pr(x|l, \boldsymbol{\Phi}_l) = \arg\max_{\boldsymbol{\Phi}_l} \prod_{i=1}^{N} Pr(\mathbf{s}_i|l, \boldsymbol{\Phi}_l) \quad (8)
$$

where $\mathbf{s} = \{\mathbf{s}_1, \mathbf{s}_2, ..., \mathbf{s}_N\}$ denotes the training dataset.

To solve the optimization problem in Eqn. 8, we adopt Expectation Maximization (EM), which iteratively optimizes the object function by two steps - E-step (*Expectation step*) and M-step (*Maximization step*). Basically, the expectation step calculates the posterior probability $Pr(l|\mathbf{s})$ by using the training dataset $\mathbf{s}$. The Maximization step maximizes the log-likelihood expectation, which in turn enables us to re-calculate the parameters in the following iteration. We use cross validation to find an optimal value of GMM component number that maximize the localization accuracy. With a learned GMM location classier, we can first calculate all the probabilities for candidate locations $\mathbf{l}_{1:G}$ given an observed $\mathbf{r}$, and then we choose the maximal one as the predicted location of the user.

4.2. k Nearest Neighbor based Localization

Another way to build a location classier is to learn the Euclidean distances of RSSI vectors under a resident appearing on a certain candidate locations. In this regard, we introduce the k nearest neighbors (kNN) method that first measures the context-dependent Euclidean distances between a testing RSSI vector with the RSSI vectors of training dataset, and then use a majority vote among its nearest neighbors to assign a location label. Specifically, assuming that we have a training dataset $\mathbf{T} = \{(\mathbf{s}_1, y_1), (\mathbf{s}_2, y_2), ..., (\mathbf{s}_N, y_N)\}$ with N samples, where $\mathbf{s}_i \in \mathbb{R}^D$ is the RSSI vector, $y_i \in \mathbf{l} = \{l_1, ..., l_G\}$ is the corresponding location label. Then, given a distance measuring method and a testing RSSI vector $\mathbf{r}$, we can search its k nearest neighbors, represented by $N_k(\mathbf{r})$. Finally, the testing RSSI vector is given a most-common location label y^* among its k nearest neighbors by following equation.

$$
y^* = \arg\max_{l_j} \sum_{\mathbf{s}_i \in N_k(\mathbf{r})} \mathbb{I}(y_i = l_j) \quad (9)
$$

where $j = 1, 2, ..., G; i = 1, 2, ..., N$ and $\mathbb{I}$ denotes an indicator function which is 1 if $y_i = l_j$, otherwise 0.

4.3. Kernel-based Localization

From the point of probabilistic view, if two RSSI vectors have a stronger similarity, then they will be in a near or even same location with a higher probability. Based on this intuition, we thus can use a Kernel-based learning (KL) to resolve the posterior probability of candidate locations given an RSSI observation. By applying a kernel function in RSSIs, KL can directly construct possible non-Euclidean topologies that are underlaid implicitly in the RSSI vectors and locations. Specifically, in the learning procedure, KL will assign the kernel with a probability mass for every RSSI vector of the training dataset. Then, for an observed RSSI vector, multiple density functions with equal weights will be utilized to estimate the probability. Mathematically, given the training data and corresponding location labels $\mathbf{S} = \{(\mathbf{s}_1, l_i), ..., (\mathbf{s}_n, l_n)\}$, we can formulate the linear-kernel based localization as the following optimization problem.

$$
\min_{\mathbf{w} \in \mathbb{R}^d, b, \xi_i} \mathbf{w}^T\mathbf{w} + C \sum_{i=1}^{n} \xi_i
$$
(10)
$$
\text{s.t. } l_i(\mathbf{w}^T\mathbf{s}_i + b) \geq 1 - \xi_i, \ \xi_i \geq 0 \ \text{for } i = 1, 2, ..., n
$$

where $\xi_i(i = 1, 2, ..., n)$ are slack variables. C means the error penalty: a small C allows constraints to be easily ignored, leading to a large margin, and a large C makes constraints hard to ignore, leading to a narrow margin. Eqn. 10 essentially is a convex optimization problem and there is a unique minimum. Based on the primal-dual relationship, we can optimize the model parameters by solving the following dual problem [30]:

$$
\begin{aligned}
\max_{\mu, \alpha} \min_{\mathbf{w}, \xi, b} \ & \mathbf{w}^T\mathbf{w} - \sum_{i=1}^{n} \alpha_i(l_i(\mathbf{w}^T\mathbf{s}_i + b) - 1 + \xi_i) \\
& + C \sum_{i}^{n} \xi_i + \sum_{i=1}^{n} \mu_i \xi_i
\end{aligned}
$$
(11)

where $\alpha = (\alpha_1, ..., \alpha_n)^T$ and $\mu = (\mu_1, ..., \mu_n)^T$ are Lagrange multipliers. After learning, in the testing stage, we can feed the RSSI observations into the trained model and output the associated location labels. In this paper, we adopt LibSVM [30] to realize the KL-based localization. Besides the linear kernel shown in Eqn. 10, there are other kernal functions such as polynomial kernel and Gaussian kernel, *etc.*. The selection of kernel function highly depends on the features of RSSI data and environmental noise causing path loss, and the shadowing and multipath effects in localization. We intensively test the linear kernel, Gaussian kernel, polynomial kernel and radial basis function kernel, finding the linear kernel works better.

4.4. Discussion

To summarize, we introduce three different types of localization methods. GMM is motivated by the jumping property of backscattered RF signal from tags, which can be explained by[350] the signal propagation mechanism. kNN is based on the similarity measurement of context Euclidean distance of observed RSSI readings. SVM (support vector machine) is an advanced classification method that are widely adopted by other localization systems. Actually, there exists other classification meth-[355] ods that can be applied into our localization system, such as Naive Bayes, Extreme Learning Machine (ELM), *etc*. We conduct some pilot experiments to compare these methods. Specifically, we first ask a subject to stand two minutes in each grids to collect the RSSI samples (the testbed is shown in Fig 5),[360] then we randomly divide the dataset into training and testing datasets in different ratios (from 10% to 90%) to test the methods. As Fig. 8 shows, among all the classification methods, k Nearest Neighbors achieve the best result. Even with only 10% training data (12 seconds in each grid), it reaches 87.2%[365] accuracy (greatly simplify the pre-calibration and relieve our training burden). It reveals that, with only a few labeled RSSI data, the context-dependent distance measurement can better interpret the fluctuation of RSSI signal caused by human body inference, which strongly motivates our kNN-HMM to tackle the tracking problem.
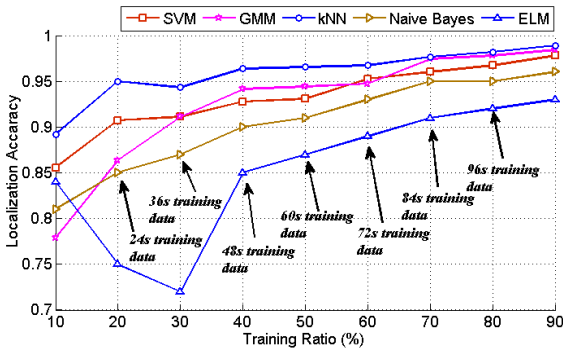

Figure 8: Localization results of different methods

5. Tracking a Moving Subject

Comparing to localizing a relatively static user, human tracking is more challenging, especially considering the sudden and[370] unpredictable RSSI changes caused by a moving human body, which makes the RSSI-Location mapping more difficult. However, on the other hand, within a sampling time, the next moving location will be near to the current location due to the human speed limitation ($\leq 1m/s$), which naturally narrows down the possible candidate locations. In other words, for tracking[375] problem, we have one more evidence, namely *current location state*, that can help us to infer the possible locations besides the RSSI observations. Specifically, we propose two HMM-based models, *kNN-HMM* and *GMM-HMM*, to decode the continuously time-stamped RSSIs into the subject's moving path by considering both patterns learned from localization model and[380]

the location transition constraints. Hidden Markov Model is widely applied in spatio-temporal pattern recognition such as handwriting recognition, proteins structure prediction and human activity recognition *etc.*. It can be considered as a generalization of a mixture model where the latent variables, which control the mixture component to be selected for each observation, are related through a Markov process rather than independent of each other. In this regard, HMM is perfectly fit the assumption of our tracking problem that the next moving location depends and only depends on present location, neither being totally independent nor related to the past location states. Another challenge in tracking is the latency, namely the subject already moves to next location whiles the system is calculating the current location. To reduce this disturbing phenomenon, given the resulting continuous location points from HMM-based models, we further design a forward calibration mechanism that substantially takes account of a few past location estimations when resolving current location. In the next, we will elaborate the details of kNN-HMM based and GMM-HMM based tracking methods as well as the forwarded calibration mechanism.

Assuming that $\mathbf{L}$ represents all candidate user's moving trajectories and $\mathbf{R}$ denotes the observed RSSI vector sequence, then our primary goal is to optimize a trajectory $\mathbf{L}^*$ with a maximum likelihood based on the following equation.

$$\mathbf{L}^* = \arg\max_{\mathbf{L}} Pr(\mathbf{L}|\mathbf{R}) \tag{12}$$

According to Bayesian Theorem, we transform optimizing the conditional distribution into finding an optimal joint probability distribution.

$$Pr(\mathbf{L}|\mathbf{R}) = \frac{Pr(\mathbf{L}, \mathbf{R})}{Pr(\mathbf{R})} \propto Pr(\mathbf{L}, \mathbf{R}) \tag{13}$$

Assuming that $\mathbf{R}$ is consisted of T time-tagged RSSI observations $\mathbf{r}_{1:T}$ and $\mathbf{L}$ contains T corresponding location states $l_{1:T}$, we can further decode Eqn. 13 as follows:

$$Pr(\mathbf{r}_{1:T}, l_{1:T}) = Pr(l_1)Pr(\mathbf{r}_1|l_1)\prod_{t=2}^{T}\underbrace{Pr(\mathbf{r}_t|l_t)}_{B}\underbrace{Pr(l_t|l_{t-1})}_{A} \tag{14}$$

Now we successfully model our tracking problem as a Hidden Markov Model. To solve the model, we first need to estimate *Transition Matrix A* and *Emission Matrix B* and then use *Viterbi Search* to find the optimal location trajectory.

- *Transition Matrix* captures state-transition probability of a user moving from a location-state l_{t-1} at time-stamp $t-1$ to a location-state l_t at time-stamp t. It can be represented via $Pr(l_t|l_{t-1})$.

- *Emission Matrix* models the probability of observing RSSI vector $\mathbf{r}_t$ given a location state l_t at time t, denoted by $Pr(\mathbf{r}_t|l_t)$.

- *Viterbi Searching* finds a location sequence $\{l_1, l_2, ...l_T\}$ that has a maximum likelihood given Transition Matrix A and Emission Matrix B.

7

5.1. Transition Matrix

First of all, we show how we build a transition matrix based on the location state constraint. Generally, the human motion can be seen as a state transition process that next moving location is solely dependent of current state but irrelevant to other states, which can be defined by a probability matrix $A_{ij} = Pr(a_t = l_i | a_{t-1} = l_j)$. To construct such a matrix, we define following two human motion patterns based on an intuition that a person is only able to move a limited distance during one sampling interval (*i.e.,* 0.5 *second* in our system) given the moving speed ($\leq 1m/s$) in an indoor environment.

- *Constraint-Less Transition (CLT):* The tracked user can move to any locations of the monitored area under a same likelihood, namely $l_t \in l_{0:G}$ with an equal probability.

- *Constraint Transition (CT):* The tracked user can only move to one-sampling-time reachable locations of the monitored area under a same likelihood and cannot reach other locations.

The second motion pattern greatly facilitates the tracking efficiency due to the fact that it can largely exclude some unlikely location states in each calculating iteration. For example, in Fig. 12, it is impossible for a resident to move from *L11* to *L64* within 0.5 second, so we can eliminate *L64* from the next moving locations whilst user's current location is *L11*. In this paper, we categorize the one-sampling-time reachable locations as those grids that are adjacent or equal to user's current location. Mathematically, we formulate these two transition patterns by one equation. We assume that the monitored area is divided into G locations and $l_i(i = 1, 2, ..., G)$ means the tracked user is in grid i. According to the proposed two motion patterns, we further define a location-state set $\mathbf{\Omega}_i$ including all feasible states that a user can move to given current state l_i, and use $|\mathbf{\Omega}_i|$ to denote the number of states. We then can construct a transition probability matrix as follows:

$$Pr(l_j | l_i) = \begin{cases} \dfrac{1}{|\mathbf{\Omega}_i|} & \text{if } l_j \in \mathbf{\Omega}_i \\ 0 & \text{if } l_j \notin \mathbf{\Omega}_i \end{cases} \quad (15)$$

5.2. Emission Matrix

As Eqn. 14 shows, $B_{ij} = Pr(\mathbf{r}_i | l_j)$ represents the emission matrix that essentially shares the same purpose as the localization problem - modeling the RSSI distributions for different location states. As a result, we can construct the emission matrix by taking advantage of aforementioned localization models.

5.2.1. GMM-based Emission Matrix

One straight-forward way is to construct the emission probability matrix based on the GMM model, which is capable of estimating emission probabilities given the RSSI observations. Similar to localization problem, we assume that the probability distribution of RSSI observations follows a multivariate Gaussian Mixture Model for each location state, and we thus are able to calculate the Emission Matrix using Eqn. 7.

5.2.2. kNN-based Emission Matrix

Another way to construct the emission matrix is taking the merit of k nearest neighbor model which reveals a superiority in mapping the RSSI observations with the latent locations. To do so, we construct a kNN-based emission matrix by transforming a traditional kNN classier into a probabilistic style that can give an emission probability conditioning on the observed RSSIs.

Specifically, the probabilistic kNN estimates the *Emission Matrix* as follows. We first search the top-k nearest neighbors $N(\mathbf{r}_j)$ in the profiling dataset for observed RSSI $\mathbf{r}_j$. Then we also mark these searched samples by its belonging locations, represented by $N^i(\mathbf{r}_j) = \{\mathbf{s}_k | \mathbf{s}_k \in \mathcal{N}(\mathbf{r}_j) \cap \mathbf{s}_k \in l_i\}$. Then the probabilistic kNN-based emission matrix is built as follows:

$$Pr(\mathbf{r}_j | l_i) = \frac{\sum_{\mathbf{s}_k \in \mathcal{N}^i(\mathbf{r}_j)}^{|\mathcal{N}^i(\mathbf{r}_j)|} \dfrac{1}{dis(\mathbf{r}_j, \mathbf{s}_k)}}{\sum_{\mathbf{s}_{k'} \in \mathcal{N}(\mathbf{r}_j)}^{|\mathcal{N}(\mathbf{r}_j)|} \dfrac{1}{dis(\mathbf{r}_j, \mathbf{s}_{k'})}} \quad (16)$$

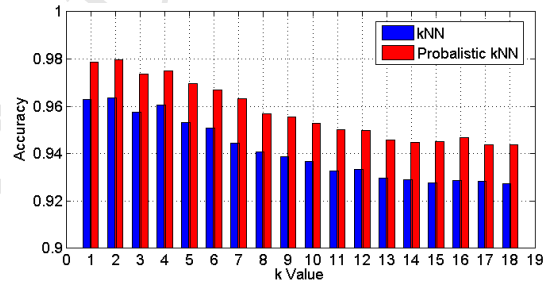where $dis(\mathbf{r}, \mathbf{s})$ represents two RSSI vectors' Euclidean distance.

Figure 9: Localization accuracy comparision with k changes

We conduct a pilot experiment to compare probabilistic kNN and transitional kNN as well. We first collect 2 minutes training data in each grid, then use 40% as the training data and 60% as the testing data to test the methods. As Fig. 9 shows, the proposed probabilistic kNN method slightly outperforms traditional kNN in all k values. More importantly, the probabilistic kNN is capable to estimate the posterior possibilities by measuring the context distances. Overall its advantages lie in: *i)* it specifically gives the posterior distribution of each class rather than assigning a class-membership to the test sample; and *ii)* it assigns each neighbor a weight that is inverse-proportional to its distance with the test sample, which not only considers the number of its most-common neighbors but also measures their relative distances.

5.3. Viterbi Searching

Given a sequence of observations, Viterbi searching, one of dynamic programming algorithms, can find an optimal sequence of hidden states with a maximum likelihood, especially being efficient in solving HMM. Specifically, assuming that the length of time-stamped RSSI observations is t and the ending location state is l_j, Viterbi searching finds the most likely sequence of latent location states as following induction process.
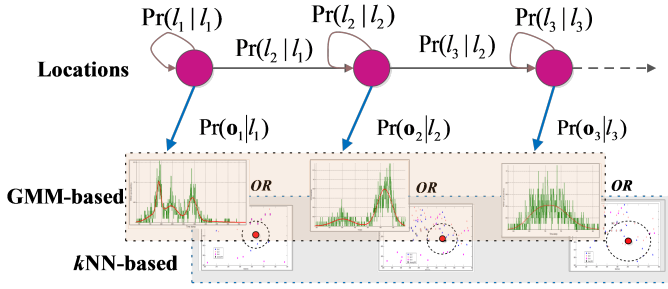
Figure 10: HMM based methods

Figure 11: Hardware deployment

$$V_j(t) = \arg \max_{l_1, l_2, ..., l_{t-1}} Pr(l_1 l_2 ... l_t = j, \mathbf{r}_1 \mathbf{r}_2 ..., \mathbf{r}_t | A, B) \tag{17}$$

where matrix A and B refer to Eqn. 14. By induction, we further obtain:

$$\begin{aligned} V_j(1) &= B_j(\mathbf{r}_1) \\ V_j(t+1) &= \arg \max_i V_i(t) A_{ij} B_j(\mathbf{r}_{t+1}) \end{aligned} \tag{18}$$

where $B_j(\mathbf{r}_1) = Pr(\mathbf{r}_1 | l_j)$ and $A_{ij} = Pr(l_j | l_i)$. After the induction calculation, we finally can search an optimal moving trajectory for both GMM and kNN based HMM methods. Fig. 10 sketches these two HMM-based methods for dealing with *Tracking*.

5.4. Latency Reduction

As aforementioned, another challenge we need to deal with in tracking is the latency, which mainly results from the delay of RSSI collection and signals sending by passive tags [28]. As a result, we introduce a *forward calibration* mechanism to re-calibrate the walking trajectory outputted by the Viterbi searching to reduce the latency. Specifically, we adopt a sliding window to average the latest several locations as follows:

$$\hat{c}'_t = \frac{\sum_{i=t}^{t+|w|-1} \hat{c}_i}{|w|} \tag{19}$$

where $\hat{c}'_t$ represents the calibrated coordinates of location l_t is the at time t, $|w|$ denotes the length of the sliding window, and $\hat{c}_i$ is raw coordinates of estimated grid's center at time i using Eqn. 17.

6. Evaluation

We evaluate our approach through *i)* micro experiments in a $3.2m \times 4.8m$ testing area (stacked by 6 RSS fields); and *ii)* field experiments in a fully furnished house including two bedrooms and a kitchen (around $220m^2$ gross floor area).

6.1. Hardware and Software Platform

Ultra-low cost of UHF tags (5~10 cents each) become the preferred choice of many industry applications. Following the common practices, we adopt passive UHF tags in this paper.
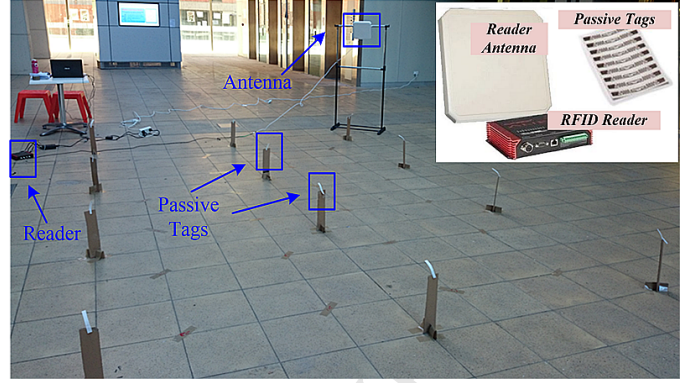
As Fig. 11 shows, our system is built upon commercial off-the-shelf RFID products without any hardware or firmware modification. Specifically, we use an Alien ALR-9900+ RFID reader, several reader-antennas (Model: ; Size: $20cm \times 20cm \times 3cm$) and dozens of UHF passive tags (Model: squiggle Higgs-4; Size: $1cm \times 10cm$). The operation frequency of the reader is 840 to 960MHz and the sampling rate is 2Hz. Each collected RSSI readings includes a TAG-ID, RSSI and TIME. Our system runs in a laptop computer (CPU: I7-3537U 2.5GHz; RAM: 8G; OS: Win7). The software for RSSI data retrieval is written by $\mathbb{C}\#$ and uses the API provided by Alien company. The back-end data analysis and modeling are based on Matlab 2016a.

6.2. Evaluation Metrics

Similar to other localization and tracking systems, we adopt the following two evaluation metrics, *Accuracy* and *Error Distance*, to measure the localization accuracy and tracking error respectively.

$$Acc. = \frac{\sum_i^N \mathbb{I}(\hat{l}_i, l_i)}{N} \tag{20}$$

where $\hat{l}_i$ and l_i respectively denote the estimated and actual location of a user, the indicator function $\mathbb{I}(a, b)$ equals to 1 if $a = b$, otherwise 0, and N denotes the tested RSSI numbers. The tracking error distance is defined by

$$D_{error} = \frac{\sum_i^{|T|} dis(\hat{c}_i, c_i)}{|T|} \tag{21}$$

The error distance depicted above actually measures the averaging accumulated error distance for each moving trajectory. Specifically, c_i and $\hat{c}_i$ mean the actual and predicted coordinates of a subject at time i, and $dis(\hat{c}_i, c_i)$ denotes the Euclidean distance between them. $|T|$ is the number of all observed RSSIs of a moving trajectory.

6.3. Micro Experiments

We first conduct several micro experiments to test our methods. Before evaluating our approaches, we need to decide how to choose the optimal size for each virtual grid. This paper aims to support the independently living for the elderly in a residential environment. So we choose the size of grids based on
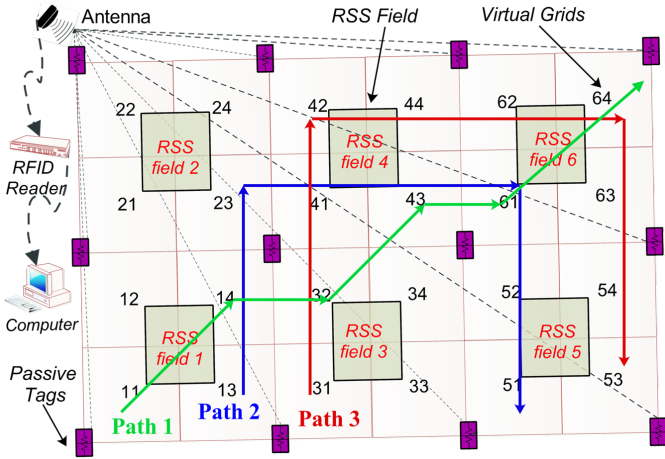
9

Figure 12: Multiple RSS fields and testing paths

Table 1: Localization accuracies of different methods by using different ratios of training data

Scena.	Ratio (%)	10	20	30	40	50	60	70	80
1	kNN	**0.946**	**0.954**	**0.958**	**0.958**	**0.960**	**0.961**	**0.962**	**0.963**
	GMM	0.927	0.935	0.938	0.940	0.939	0.943	0.940	0.941
	SVM	0.707	0.756	0.823	0.851	0.897	0.912	0.919	0.928
	ELM	0.664	0.764	0.719	0.771	0.881	0.898	0.904	0.904
	NaiveBayes	0.883	0.887	0.913	0.930	0.938	0.944	0.943	0.946
2	kNN	**0.810**	**0.823**	**0.833**	**0.844**	**0.869**	**0.902**	**0.913**	**0.931**
	GMM	0.751	0.777	0.783	0.793	0.838	0.884	0.894	0.902
	SVM	0.656	0.717	0.775	0.797	0.819	0.832	0.846	0.857
	ELM	0.680	0.538	0.614	0.701	0.677	0.774	0.819	0.835
	NaiveBayes	0.741	0.777	0.793	0.844	0.872	0.890	0.903	0.914
3	kNN	**0.880**	**0.904**	**0.918**	**0.927**	**0.931**	**0.931**	**0.936**	**0.943**
	GMM	0.851	0.877	0.883	0.893	0.898	0.904	0.904	0.912
	SVM	0.715	0.746	0.774	0.826	0.840	0.854	0.876	0.881
	ELM	0.688	0.583	0.617	0.693	0.705	0.812	0.840	0.846
	NaiveBayes	0.768	0.789	0.855	0.889	0.918	0.921	0.928	0.929

the requirement of a specific application. Based on our experiments, a grid with too small size (*e.g.,* $0.1m \times 0.1m$) would increase the calculation overhead and need more profiling data (for training the model), because a small grid size brings more indistinguishable patterns. On the other side, a grid with too large size (*e.g.,* $2m \times 2m$) may lead to a coarse-grained localization, for example, a regular bedroom with 10 square meters can only be divided into 2 grids, leading to a room-level localization. As a result, we need to wisely choose the grid size based on the specific requirement of a real-world application. In this paper, a very high location resolution is not our primary goal. For example, caregivers normally more concern about the elderly resident locating on which area or room of a house or apartment instead of an extremely fine-grained location point. Based on this intuition, we setup our experiments as Fig. 12, in which each virtual grid is $0.8m \times 0.8m$, locating people in a $0.64m^2$ resolution.

6.3.1. Experimental Settings

As Fig. 11 shows, one reader-antenna is placed at $1.55m$ height and faces to passive tags from $25° \sim 75°$ angle[7]. The tags are attached on paperboard-holders placed $30cm$ above the ground. Considering that our model aims to learn the RSSI-Location mapping, those passive tags can be flexibly put as any geometric shape. For simplicity, we deploy the passive tags as a square array with around $1.6m$ distance. Another issue is that, the reader may lose some RSSI readings due to the human body occlusion during localization or tracking. As a result, to make the received RSSI vector with same number of readings, we fill in those missing values as 0 in each sampling time.

6.3.2. Localization

To test the localization capability, we define three scenarios to simulate the possible real-world daily routines.

Scenario 1 (Stationary). *A person stands or sits statically in a certain location of monitored area, mimicking that a resident may talk with someone or watch TV.*

Scenario 2 (Dynamic). *A person moves around and does several activities within a certain small zone, mimicking a resident may cook in the kitchen or do morning exercise.*

Scenario 3 (Mixed). *A subject performs both activities defined in Scenario 1 and 2 within a certain location.*

Accordingly, we test our system based on the above three scenarios: *i)* a participant appears in each location for $120s$; *ii)* a participant walks around and performs some activities in each grid for $120s$; and *iii)* a participant does the above activities for $240s$ per grid. Overall we collect 276,480 RSSI readings in the localization experiments. We randomly split it into testing and training datasets based on different ratios (in each ratio, we run the methods twenty times to calculate the average localization accuracy). Table 1 compares our experimental results of five localization methods with different training ratios. We carefully tune the parameters for each method - we set $k = 2$ for kNN and GMM component number as 4, and choose termination criterion and C in SVM with a linear kernal as 0.01 and 1 respectively [30]. For a stationary scenario, all five methods can localize the subject with a decent accuracy. Among all, kNN classifier achieves a 94.6% localization accuracy in particular with $12s/grid$ training data, which significantly outperforms other methods especially the SVM and ELM. For a challenging dynamic localization scenario, kNN still achieves a better performance with 93.1% accuracy using 80% training data. It is also noted that, under a *dynamic* scenario, the localization accuracy is more relevant to the training data size. A larger training dataset is able to provide more informative RSSI patterns for this case. In Scenario 3, our system is able to reach a high accuracy of 94.3%. In summary, under a circumstance of limited training data (*e.g.,* 10% training data), kNN based localization reveals a better and robust performance. It is worth to mention that, to achieve a similar accuracy, the shortest collection time of training data is of *minutes-level* in past localization systems [31]. On the contrary, our system only requires a *seconds-level* collection time to get a comparable localization performance. We also observe that, with more training data (*e.g.,* 80% training data in Table 1), other methods are also able to get good accuracy but more sensitive to the training data size.

---

[7]The antenna angles or height can be set up arbitrarily as long as it is able to capture all the readings of all tags in an empty environment.
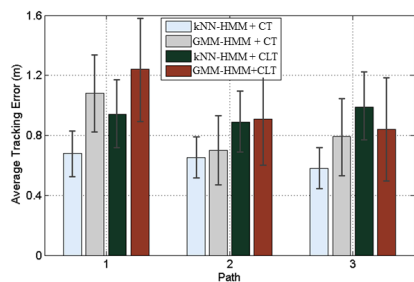
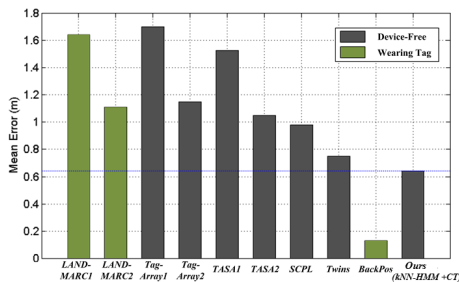Figure 13: Tracking errors on three paths (*CT: Constraint Transition; CLT: Constraint-Less Transition*)
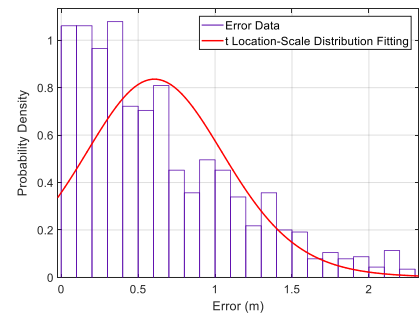

Figure 14: Average tracking errors

Figure 15: The error data and *t* Location-Scale Distribution fitting for kNN-HMM + CT

6.3.3. Tracking

In the tracking experiments, we evaluate our HMM based models on three moving trajectories[8] under the proposed two transition strategies, illustrated in Fig. 12. Two persons with various weights and heights participate our experiments and every path is tested for 20 times[9]. As Fig. 13 illustrates, kNN-HMM with Constraint Transition (*i.e.,* kNN-HMM + CT) is able to track a subject with $0.64m$ mean error, achieving the best result among all the methods. This may lie in the fact that kNN-HMM + CT feasibly narrows down the candidate locations (excluding the invalid location candidates), thus can better quantify the mapping relation from RSSI sequence to moving trajectories. We also compare our system with other popular RFID-based localization works, as shown in Fig. 14.

LANDMARC [4] is the very first RFID-based localization system that tracks a tagged subject by measuring its weighted average locations of its nearest four tags. It needs the target attached with tags and know the reference tags' locations. In our experimental testbed, it achieves average tracking error $1.64m$ (*i.e.,* LANDMARC-1: 3×4 reference tags with $1.6m$ interval), and $1.11m$ (*i.e.,* LANDMARC-2: 5×7 reference tags with $0.8m$ interval).

TagArray [11] is one of the first RFID-based systems that can localize a subject in a device-free manner. Generally, TagArray detects a person by comparing the variation of RSSI readings with a pre-learned threshold. However it is built upon active RFID tags and requires a high tag tensity as a tag array. It reaches $1.7m$ (*i.e.,* TagArracy-1: 3×4 reference tags with $1.6m$ interval) and $1.15m$ (*i.e.,* TagArray-2: 5×7 reference tags with $0.8m$ interval) mean tracking error in our testbed.

TASA [10] is another device-free RFID-based localization system, which adopts both passive and active tags. Thus it is less costly than TagArray. But still, it requires to calibrate all tags' coordinates. It gives $1.53m$ (*i.e.,* TASA-1: 3×4 reference tags with $1.6m$ interval) and $1.05m$ (*i.e.,* TASA-2: 5×7 reference tags with $0.8m$ interval) mean tracking error.

SCPL [9] is one of the advanced wireless-based device-free localization systems. It utilizes a Gaussian model based Conditional Random Field (GM-CRF) method to track a moving person. It is very similar to our GMM-HMM method (utilizing Gaussian Mixture Model). We implement the GM-CRF method in our RFID dataset and get a mean $0.98m$ tracking error.

Twins [22] is a very recent RFID-based system purely built upon passive tags, which utilizes a interference phenomenon (called state jumping) of two passive RFID tags to do the motion detection. It gives a mean $0.75m$ tracking distance error in an open warehouse. Twins also needs to carefully calibrate the positions of the reference tags.

BackPros [7] is one of the recent RFID-based positioning systems, which is able to track a passive tag with a decimeter-level accuracy. However, BackPro aims to track an object instead of tracking a human body by exploring the phase differences of backscatter signals to infer the tag's location. It needs to carefully calibrate the positions of four antennas beforehand and the tracked object need to be attached with a passive tag.

Different to the baseline methods, our system does not need to calibrate the tags' locations[10] and achieves $0.64m$ average tracking error in our testbed. It offers about 2.56×, 2.66×, 2.39× and 1.53× improvement compared with LANDMARC [4], TagArray [11], TASA [10], SCPL [9] (see Fig. 14) using the same number of tags. Fig. 20 shows the CDF (cumulative distribution function) curves of tracking error for different methods. The kNN based HMM with CT achieve a better result, nearly 76% tracking errors are below $1m$.

6.3.4. Evaluation by t Location-Scale Distribution Fitting

In this section, we compare our system with baseline methods in terms of *t* Location-Scale Distribution Fitting. This idea is first introduced by [32]. The author argue that, for a small testing dataset, it is necessary to adopt a performance evaluation criteria that can approximate the actual performance of system in practice. Similar to the *t*-distribution fitting based method proposed in [32], in this paper we first utilize *t* Location-Scale Distribution (an extension of *t*-Distribution) to fit those error

---

[8]During the experiments, we do not specifically require the testing participants to walk through the centre of each grid, we just set predefined trajectories and each trajectory is composed by several grids, which is later used as ground truth labels for model evaluation.

[9]We mainly focus on tracking a resident with a moderate moving speed ($\approx 0.6m/s$) due to that fast moving in an indoor environment is not practical.

---

[10]Although we put tags in a square array in Fig. 12, we actually do not use any coordinates of the tags. Because we target to learn the mapping model, the tags can be placed in other geometric locations.
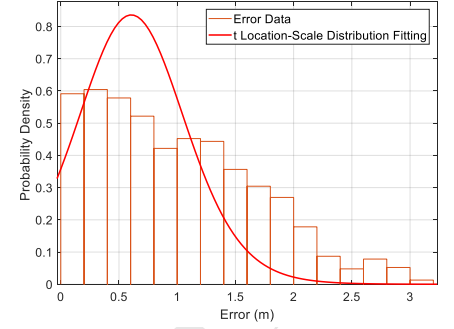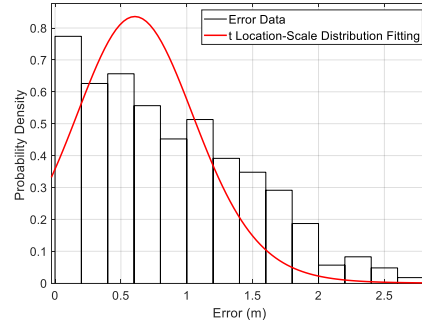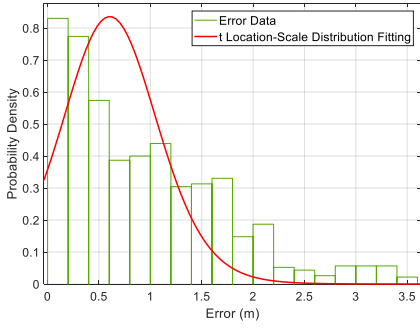
Figure 16: The error data and *t* Location-Scale Distribution fitting for kNN-HMM + CLT

Figure 17: The error data and *t* Location-Scale Distribution fitting for GMM-HMM + CT

Figure 18: The error data and *t* Location-Scale Distribution fitting for GMM-HMM + CLT
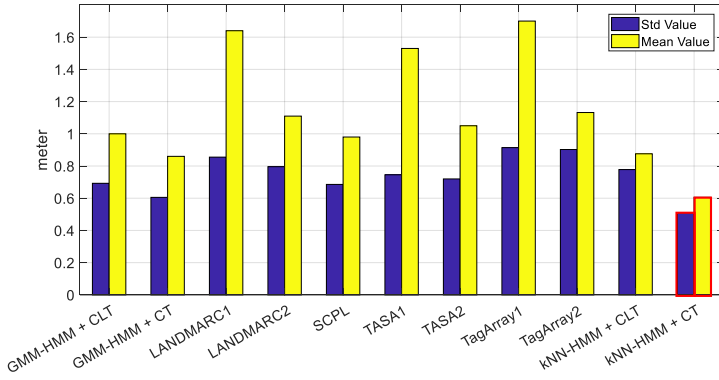

Figure 19: The stand derivation and mean value of *t* Location-Scale Distribution fitting for baseline methods
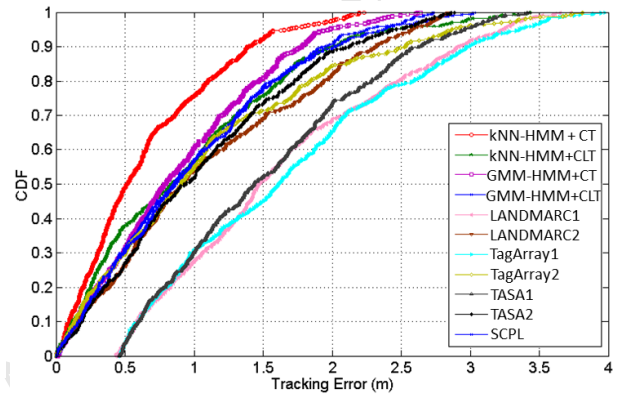

Figure 20: Tracking error CDF

datasets produced by different localization methods. Then we compare the standard derivation and mean values of those distributions fitted.

The probability density function (PDF) of the *t* location-scale distribution **??** is

$$f(r_{err}) = \frac{\Gamma(\frac{\nu+1}{2})}{\mu\sqrt{\nu\pi}\,\Gamma(\frac{\nu}{2})} \left(1 + \frac{(r_{err} - \mu)^2}{\sigma^2\nu}\right)^{-\frac{\nu+1}{2}} \quad (22)$$

where r_{err} indicates the error data, $\Gamma(*)$ represents the gamma function, μ is the location parameter and σ means the scale parameter, ν is the shape parameter. Actually, we can transfer *t* location-scale distribution into a Student's *t*-distribution when parameters $\mu = 0$ and $\sigma = 1$.

Fig. 15 $\sim$ 18 illustrate the probability densities along with error distances for kNN-HMM + CL, kNN-HMM + CLT and GMM-HMM + CL as well as kNN-HMM + CLT, and the corresponding *t* location-scale distributions fitted. Fig. 19 shows the standard derivation and mean values of the distributions for all the compared methods. As we can see, the proposed method, kNN-based HMM with Constraint Transition, achieves a lower mean and standard deviation values.

6.4. Field Experiments

This section delivers the experimental results in a residential house that contains 2 bedrooms (*i.e.,* a home office and a master room) and a kitchen, as shown in Fig. 24. The reader-antennas are deployed around 1.7 *meters* vertical distance to the ground

and the facing angle to the passive tags is around 60 °, which is capable of capturing all RSSI readings under a non-resident environment. Overall we virtually divide the monitored area into 25 grids, and use 34 passive RFID tags and one reader with three antennas. We attach those passive tags on the room-walls with about 0.8*m* interval.

6.4.1. Localization

Similarly, we design three localization scenarios in our field experiments - *Stationary*, *Dynamic* and *Mixed*. Accordingly, three types of data are collected to train and test the location classifiers[11].

Figure 21∼23 show the results of localizing a subject using five different location classifiers varying training ratios (from 5% to 90%)[12]. In the *stationary scenario*, the localization accuracy of *k*NN is as high as 93.8% with 90% training ratio. More importantly, only with 6 seconds training data (5% training ratio) for each grid, it can achieve an accuracy over 85% in a residential house, revealing its advantage than other location classifiers. For Scenario 2, the performances of all methods are

---

[11] *i)* a person appears in each grid for 120*s*, *ii)* a person contentiously moves round in a grid for 120*s*, and *iii)* a participant does the above stationary and dynamic activities respectively for 120*s*. For L1, L10, L11, we only collect the data people lying down for all scenarios. Overall, we collect 848,640 RSSI readings, forming 24,960 RSSI vectors.

[12] We randomly choose the training dataset and testing dataset, and conduct each experiments 20 times, reporting the average accuracies
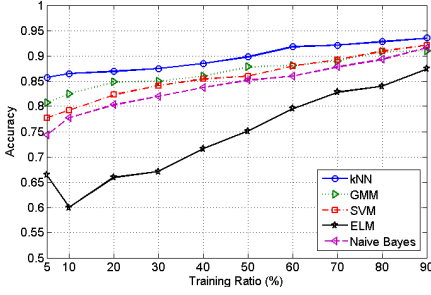
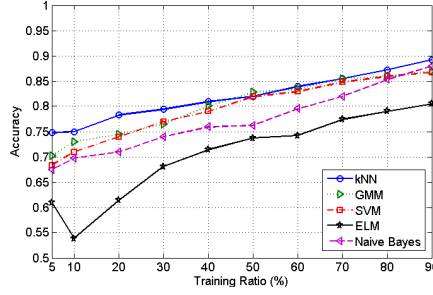Figure 21: Localization accuracy in Senario 1

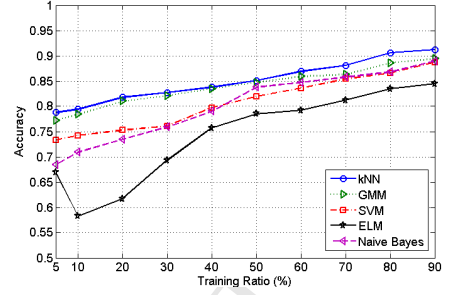Figure 22: Localization accuracy in Senario 2

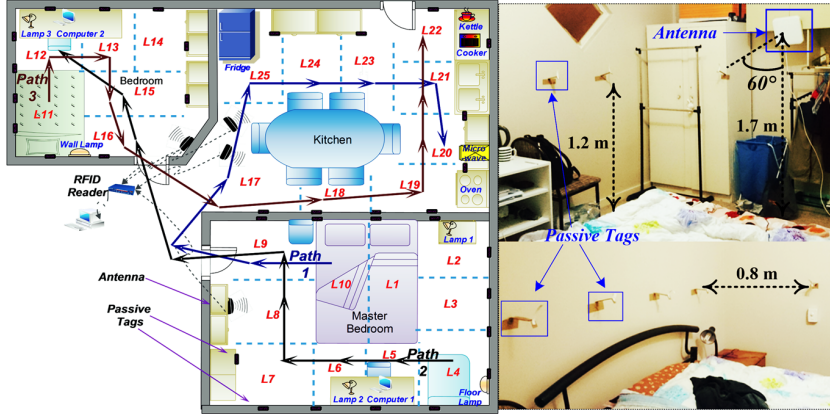Figure 23: Localization accuracy in Senario 3
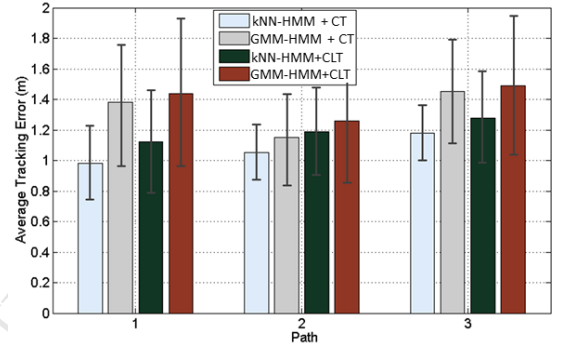

Figure 24: House layout and tracking paths

Figure 25: Tracking errors on three paths

degenerated due to the unstable human inference, and the results among different methods are more close to each other. We also observe that more training data can significantly enhance the localization accuracy, which means, for the challenging *dynamic scenario*, collecting more training data can more accurately capture the human inference to RSSI signals. For Scenario 3, the best perfermance is achieved by kNN using 90% training data, and the overall performance is between *stationery scenario* and *dynamic scenario*. In summary, kNN shows its superiority in RFID-based device-free localization, considering its simplicity, light computation overhead and relaxing requirement of training data.

6.4.2. Tracking

We also test our tracking methods on three daily routines, shown as Fig. 24.

Path 1: $L10 \rightarrow L9 \rightarrow L17 \rightarrow L25 \rightarrow L24 \rightarrow L23 \rightarrow L21 \rightarrow L20$ represents that, a resident gets up from the master room and does some cooking in the kitchen.

Path 2: $L4 \rightarrow L5 \rightarrow L6 \rightarrow L7 \rightarrow L8 \rightarrow L9 \rightarrow L16 \rightarrow L15 \rightarrow L12$ mimics that a resident gets up from the sofa $L4$ of the master room, and then goes to work at the desk $L12$ of the home office (*i.e.,* the room in the upper-left of Fig. 24).

Path 3: $L11 \rightarrow L12 \rightarrow L15 \rightarrow L16 \rightarrow L17 \rightarrow L18 \rightarrow L19 \rightarrow L20 \rightarrow L21 \rightarrow L22$ indicates that, a resident gets up from the bedroom and goes to the kitchen using the kettle.

Overall three subjects join the experiments and each path test is repeated 20 times. As Fig. 25 depicts, our proposed kNN-HMM with Constraint Transition illustrates a better result (with $1.07m$ mean tracking error) comparing to other HMM based

models. It is noted that, in Path 3 - a more complex path of daily routine, our method obtains a larger tracking error (nearly $1.2m$). The reason may be due to the fact that Path 3 involves walking through a narrow hall with many electronic appliances in the kitchen, which block or absorb the energy of backscattered signal from an antenna. Thereby the tracking accuracy decays for this application scenario. In general, our proposed method outperforms other methods by intensively learning the mapping relation between RSSI readings and human mobilities under a transition constraint. It is noted that SCPL achieves $1.66m$ mean error, 1.55 times larger than our method. In the field experiment, we only compare our system with the proposed method in SCPL since the LANDMARC, TagArray and TASA place the RFID tags as arrays on the ground. Such deployments are impractical and obtrusive for a residential environment. Firstly, the reader even cannot catch the readings from passive tags that are deployed in a carpet ground since signals are blocked by furnitures around and absorbed by the carpet. Secondly, tag-arrays that densely deployed on ground in a residential environment strongly obstructs the mobility of the resident, causing uncomfortable and inconvenient. In our system, the passive tags are attached on the wall which is more practical and considered as less intrusion. As a result, the localization systems proposed in LANDMARC, TagArray and TASA are no longer capable for the residential application scenario.

6.5. Parameters Selection

In this section, we will discuss the factors that have impact on the tracking accuracy.

13

6.5.1. Tag Density

Tag density is an important influential factor to the tracking performance. As Fig. 26 shows, we investigate the impact of tag density by deploying different numbers of tags in the testing rooms. The experiments reveal that a sparse tag density (*e.g.,* 2 tags/room) will reduce the tracking performance. On the other side, continuously using more passive tags does not improve the tracking accuracy significantly. For example, in our experiments, the tracking error does not decrease obviously when increasing the tag number from 34 to 89. Such a phenomenon lies in a fact that it is difficult for an antenna to probe a large number of passive tags and thus resulting in severe reading loss. It is noted that, comparing to TagArray and TASA that require a high density of tags, our system is able to achieve a comparable tracking accuracy using less passive tags.

6.5.2. k Value and GMM Component Number

There are two key parameters in our HMM-based models, one is k value in Emission Matrix of kNN-HMM, another one is the *component number* (CN) of GMM in GMM-HMM. We investigate these two parameters in our micro experiment testbed. Fig. 28 illustrates that, the tracking error reaches the lowest when $k = 7$, which thus is chosen as the optimal value in our tracking system. However, GMM-HMM achieves a better tracking accuracy at CN = 4, 8, 9 and 15. Considering that a larger CN may potentially cause a model over-fitting and requires more computation overhead, we choose CN = 4 in this paper.

6.5.3. Window Length

For a localization system, dealing with the latency is also a concerning issue [33, 1]. In this paper, we introduce a simple yet efficient forward calibration to reduce the latency, laying on the fact that previous human motion has an impact on current location prediction. One of key parts is to decide the length of *previous motion*, *i.e.,* the smoothing window length. Fig. 29 shows the relevance between the window size of forward calibration and the tracking error in different paths using two HMM based methods. We observe that, when the window length ranges from 8 to 11, our system achieves a less tracking error. Thus, we select 8 as the optimal length in our system considering both the computational burden and accuracy.

6.5.4. Stationary Data vs Dynamic Data

As mentioned before, we put two kinds of training data into the HMM based methods - stationary data (Scenario 1) and dynamic data (Scenario 2). In order to analyze which type of training data plays a key role in tracking, we first add 120 seconds *dynamic* training data (before black dot line, *the First-stage Training*), then we add another 120s stationary data for training (after black dot line, *the Second-stage Training*), shown as Fig. 30. Overall, we observe that the tracking error decreases as adding more training data. In details, the error diminishes rapidly in the first stage, but just slightly reduces in the second stage. Actually, the last 72 seconds stationary data does not make much contribution to improving the performance. It reveals that more dynamic data substantially provide richer anchoring RSSI information regarding the human motion, and a few stationary training data (*e.g.,* collecting 24 seconds training data) nearly provide all the essential statical information for tracking. In other words, we can add more dynamic training data to improve the system's tracking performance.

6.6. Computation Complexity

The proposed traking method is based on the framework of Hidden Markov Model and use a Viterbi Searching to decode the user's trajectories. The complexity of our algorithm is $O(T \times S^2)$, where T is the number of RSSI vectors observed and S is the number of location states, which is 26 in the field experiments. Thus our algorithm has a linear complexity with respect to the length of observations, which is efficient enough given the advances of current COTS computers. Actually, some baseline methods such as LANDMARC is simpler, which is only based on k Nearest Neighbors without any dynamic programming algorithms for sequence matching.

7. Related Work

This section will review the related works regarding indoor localization and tracking. Generally, they can be categorized as *wearable-device based localization* and *device-free localization*. We will focus more on the device-free techniques that is more related to our system.

7.1. Wearable Devices based Localization

Wearable device based systems normally requires the user to carry or wear a device such as RF transceivers, smart-phones, RFID reader or tags. The very first indoor localization work is Criket [39] which is able to track a subject wearing an ultrasonic transmitter by measuring the ToA (time-of-arrival) of a short ultrasound pulse. Another very famous pioneering work, LAND-MARC [4], first deploys dozens of active RFID tags in the indoor environment, and then match the RSSI from a tag carried by a subject with the profiled RSSI fingerprints to localize a target. Lately, Yang et al. [6] design a high-performance tracking system based on passive RFID hardware, which can real-time track a tagged object with a centimeter-level error. With the popularity of smart phones, Zhou et al. [40] present an activity sequence-based pedestrian indoor localization approach using smartphones. They first detect the activity sequence using activity detection algorithms and use HMM to match the activities in the activity sequence to the corresponding nodes of the indoor road network. MaLoc [41] utilizes magnetic sensor and inertial sensor of smart-phones by a reliability-augmented particle filter to localize a subject, which does not impose any restriction on smart-phones orientation. Currently, wearable device based localization is still a very active research area due to its high accuracy and robustness. However, the requirement of wearing a sensor or device may be not practical for some circumstances.

Table 2: Comparison of typical device-free localization systems

Comparison Systems	Measured Physical Quantity	Non-LoS Localization?	Hardware	Cost of Single Node/Device	Localization Accuracy	System Scalability	Maintenance (*e.g.,* replace battery *etc.*)	Training Overhead	Tested in a Residential Home?	Device -free?
TagArray[11]	RSS Threshold	NO	Active Tags	Medium	Medium	Medium	Medium	Low	NO	YES
TASA[10]	RSS Threshold	NO	Passive and Active Tags	Medium	Medium	Low	Medium	Low	NO	YES
RTI[17]	RSS Attenuation	NO	Wireless Nodes	Medium	High	High	High	Low	NO	YES
CareLoc[34]	Swipe Event	NO	Passive RFID Tags	Low	High/Detecting Swipe Event	High	Low	Low	NO/Test in Hospital	NO
NUZZER[35]	RSS Changes	YES	Wireless Nodes	Medium	High	Medium	Medium	High	NO	YES
SCPL[9]	RSS Changes	YES	Wireless Nodes	Medium	Medium	High	Medium	Medium	NO	YES
ilight[36]	Light Strength	No	Light Sensors	High	Medium	Low	Medium	Low	NO	YES
Ichnaea[18]	RSS changes	YES	Wireless Nodes	Medium	High	High	Medium	High	NO	YES
Twins[22]	Critical State Jump	YES	Passive Tags	Low	High	Medium	Low	Low	NO	YES
VisualLoc[37]	Video Frame	NO	Wireless Visual Sensors	High	Very High	Medium	Medium	Low	No	YES
WiTrack[21]	FMCW signal	Yes	USRP	Very High	Very High	Medium	High	Low	NO	YES
FlexibleTrack[38]	RSSI	YES	Smartphone and Wireless Nodes	Medium	Medium	High	Medium	Low	NO	NO
Ours	RSS Variance	YES	Passive Tags	Low	High	High	Low	Low	YES	YES

7.2. Device-free Localization

On the contrary, device-free technique can relax such wearing requirement for users. In 2007, the device-free localization challenge is first identified by Youssef et al. [3] who have designed a preliminary WIFI-based DfP localization system. Since then enormous DfP localization schemes have emerged. Basically, according to the type of hardware installed, device-free localization schemes can be generally classified into three categories: WIFI, RFID, and environmental sensors[13] based techniques. Based on the techniques of dealing with localization and tracking, the methods can be categorized into model-based (*e.g.,* RTI [43], FREDI [44], TASA [10]) and fingerprint-based (*e.g.,* LANDMARC [4], SCPL [9], WILL [5]). Environmental sensor based category includes many types of sensors, which either cost too much or need some special deployment for facilities, or sensitively be influenced by natural light or thermal source. In the next, we will intensively review the device-free localization systems based on WIFI and RFID.

7.2.1. WIFI-based Device-free Localization

With the pervasiveness of WIFI, enormous device-free localization systems built upon wireless signals have been emerged during last decade [1]. The general intuition behind this technique is that, when a user moves in a monitored area, RSS and CSI abstracted from WIFI signals will embody different attenuation levels. WIFI-based schemes exploit various models to decode the signal variations in either RSS or CSI for localization or tracking [8]. For example, RTI [17] proposes a radio tomographic imaging (RTI) model to resolve the RSS attenuation caused by human motion within an area with dense-deployed wireless notes. By extending the fingerprint-based technique, Xu et al. [31] adopt various several discriminant analysis approaches to classify a user's location. Furthermore, they design another localization system, SCPL [9], which is able to count

and localize multiple residents. Later on, NUZZER, a large-scale indoor DfP tracking system, is developed by Seifeldin et al. [35]. This work first builds a passive RF map in an off-line manner and then utilize a Bayesian model to find a location with maximum likelihood. Ichnaea [18] is another advanced WIFI-based device-free system in terms of training overhead and robustness. It combines anomaly detection method and particle filtering to robustly track a single subject in an area with wireless infrastructure. Recently, WiTrack, designed by Adib *et al.* [21], is able to track a human body even the subject is behind a wall or occluded by furnitures. It requires the support of USRP and decodes the locations by analyzing the reflected specialized Frequency Modulated Continuous Wave from the human body.

Moreover, given the pervasiveness of fingerprinting-based techniques applied in the indoor localization, many researchers focus on improving accuracy in the fingerprintbased indoor positioning. In [45], Akis *et al.* introduce a Route Probability Factor (RPF) to model the possibility of proximal points within the user's moving trajectories, which essentially adopts the map constraints as priori information to improve the performance of localization. Loizos *et al.* recently propose a Sample Size Determination Algorithm (SSDA) that explores confidence levels and standard deviation in a small testing dataset to approximate the actual performance of the system. SSDA can furthermore estimate the minimum data sample size needed for a fair performance evaluation for fingerprint-based systems. Some survey papers such as [46] intensively review those emerging fingerprinting-based solutions and identify some new evaluation metrics and challenges for the performance comparison of indoor localization.

7.2.2. RFID-based Device-free Localization

Undoubtedly, WIFI-based systems bear some promising characters such as moderate cost, tiny node size and elegant signal propagation models. However, they still require to be powered in a wire or battery style, which inevitably need regular maintenance, *e.g.,* periodical replacement of batteries. On the contrary, RFID-based DfP localization systems have shown

---

[13]For simplicity, in this paper, we generally treat camera-based techniques as one type of environmental sensors, including infrared sensors [15], light sensors [36, 42], and varies kinds of cameras [13, 14, 16]

more attractive features such as significant cost-efficiency, zero maintenance (cheap passive tags) and good hardware scalability. Thus several pioneering device-free systems have been developed recently based upon either active or passive RFID hardwares. The very first RFID-based device-free localization system, TagArray, is proposed by Liu et al. [11] who place active RFID tags as arrays on the ground localizing a subject by measuring if RSSI readings are higher than a threshold. TASA [10] is another similar device-free localization system but is more cost-efficient due to it utilizes both passive and active RFID tags. Both TagArray and TASA systems focus more on mining frequent trajectory patterns instead of tracking accuracy, and they only quantify the binary relation of RSSI readings with human locations (*i.e.,* comparing RSSIs with thresholds). Later on, Wagner et al. [47] extend the RTI model from WIFI-based localization to RFID hardware platform that can track a single user in a small obstacle-free zone with dense passive tags deployed. Very recently, a new localization system built upon passive tags, Twins [22], is also proposed, which leverages an interference observation of two very-near tags to detect an intruder in a warehouse reaching $0.75m$ mean tracking error. Table 2 compares our system with other typical localization systems in a high-level view. Our work thoroughly mines the relations between the RSSI of tags and the impact brought by human motion to achieve high accuracy localization and tracking. Moreover, our RFID-based system is built *solely* upon passive tags, which is less costly and more convenient for a practical deployment (*e.g.,* tiny size and weight, battery-free feature). At the same time, our system does not contain any privacy information since it merely exploits RSSI signals from passive tags.

8. Conclusion

Indoor localization and tracking systems built upon passive RFID hardware have shown attractive potential of passive tags due to the cheap price, low-maintenance and battery-free character. Those promising features strongly motivate this paper, in which we design, implement and evaluate an RFID-based DfP indoor localization and tracking system built upon passive tags. By taking advantage of supervised classification methods, we introduce a series of data-driven models to quantify the RSSI distributions when a user appears at various locations within a monitored area. These approaches enable our system to localize a subject by maximizing the posteriori probability given RSSI observations. To transfer the pattern learned in localization into tracking, we further propose the multivariate GMM-based HMM and kNN-based HMM methods, in which we utilize the probabilistic estimation learned in localization to construct the emission matrix and introduce two human mobility strategies to approximate the transmission matrix under the hidden Markov assumption. The intensive experimental results verify the effectiveness and accuracy of our system.

In the next, we will discuss several practical issues in our system that are left for the future work.

Data-driven Method vs. Physical Model: This paper introduces a series of methods from a data-driven viewpoint to

deal with human localization and tracking problems. Comparing with physical models that leverage the backscatter propagation mechanism, it delivers many promising features including no requirement of tag pre-calibration, flexible deployment of RFID tags, a large monitoring area, and robustness in the face of multi-path effect[14]. However, a learning/training stage is necessary. Based on our experiments, for a $20m^2$ room, it requires about one-minute training data to reach 85% in accuracy. Future work in this regard will focus on the investigation of how to utilize the signal's backscatter propagation to facilitate our data-driven model for further reducing the learning overhead.

Tracking Multiple Residents: Our system targets to track a single resident in an indoor environment with an aim to support independent living for the elderly. For the circumstance of several residents locating in a same residential room, the location-RSSI impacts from different persons will be tangled and coupled which require an expensive learning overhead, *i.e.,*, exponentially increasing with the number of residents. One way to address this problem is to retrieve other information from the backscatter signals in RFID tags such as RF phase, RSSI reading rate, doppler frequency. These signal information can potentially serve as indicators of locations and reduce the pattern overlapping from multiple users, thus to ease the learning burden. In the future, we will investigate this idea in details.

Locations of Tags: Tag's location is an important influential factor to the localization accuracy, especially for non-fingerprint based methods. In this paper, we use a data-driven method to model the relationship of RSSI with locations, which means we are quite flexible to the tags locations as long as the RF signal from antenna to tags can cover the whole monitored area. Exploiting how tags locations and numbers influence the accuracy in a specific application scenario, such as indoor localization and human activity recognition, is also an interesting direction in the future.

Why Not Deep Learning: Deep Learning (DL) now is a powerful and state-of-the-art supervised learning tool in many communities, especially in computer vision, speech recognition *etc.*. However, Our system is built upon the passive RFID hardware, which substantially produces low-dimension RSSI data (*e.g.,* 12 or 34 dimensions in our application scenarios) and the training dataset is relatively small and limited. As a result, given the low-dimensional and limited training dataset, as well as a fact that traditional methods can achieve good performances, we do not adopt the deep neutral network in this paper. However, how to introduce or apply DL techniques into the sensor network community is an interesting and promising future direction as well.

References

[1] Z. Yang, Z. Zhou, Y. Liu, From rssi to csi: Indoor localization via channel response, ACM Computing Survey 46 (2) (2013) 25:1–25:32.

---

[14]Data-driven methods substantially learn the multi-path effect directly in the model-training stage instead of designing a delicate multipath propagation model in physical model based methods.

[2] C. Luo, H. Hong, L. Cheng, M. C. Chan, J. Li, Z. Ming, Accuracy-aware wireless indoor localization: Feasibility and applications, Journal of Network and Computer Applications 62 (2016) 128–136.

[3] M. Youssef, M. Mah, A. Agrawala, Challenges: Device-free passive localization for wireless environments, in: Proceedings of the 13th Annual ACM International Conference on Mobile Computing and Networking (MobiCom 2007), 2007, pp. 222–229.

[4] L. Ni, Y. Liu, Y. C. Lau, A. Patil, LANDMARC: indoor location sensing using active rfid, in: Proceedings of the First IEEE International Conference on Pervasive Computing and Communications (PerCom 2003), 2003, pp. 407–415.

[5] C. Wu, Z. Yang, Y. Liu, W. Xi, WILL: Wireless indoor localization without site survey, in: Proceedings of the 31st IEEE International Conference on Computer Communications (INFOCOM 2012), 2012, pp. 64–72.

[6] L. Yang, Y. Chen, X.-Y. Li, C. Xiao, M. Li, Y. Liu, Tagoram: Real-time tracking of mobile rfid tags to high precision using cots devices, in: Proceedings of the 20th Annual International Conference on Mobile Computing and Networking (MobiCom 2014), 2014, pp. 237–248.

[7] T. Liu, Y. Liu, L. Yang, Y. Guo, W. Cheng, Backpos: High accuracy backscatter positioning system, IEEE Transactions on Mobile Computing PP (99) (2015) 1–1.

[8] Z. Yang, C. Wu, Z. Zhou, X. Zhang, X. Wang, Y. Liu, Mobility increases localizability: A survey on wireless indoor localization using inertial sensors, ACM Computing Survey 47 (3) (2015) 54:1–54:34.

[9] C. Xu, B. Firner, R. S. Moore, Y. Zhang, W. Trappe, R. Howard, F. Zhang, N. An, SCPL: Indoor Device-free Multi-subject Counting and Localization Using Radio Signal Strength, in: Proceedings of the 12th International Conference on Information Processing in Sensor Networks (IPSN 2013), 2013, pp. 79–90.

[10] D. Zhang, J. Zhou, M. Guo, J. Cao, T. Li, Tasa: Tag-free activity sensing using rfid tag arrays, IEEE Transactions on Parallel and Distributed Systems 22 (4) (2011) 558–570.

[11] Y. Liu, Y. Zhao, L. Chen, J. Pei, J. Han, Mining frequent trajectory patterns for activity monitoring using radio frequency tag arrays, IEEE Transactions on Parallel and Distributed Systems 23 (11) (2012) 2138–2149.

[12] W. Ruan, L. Yao, Q. Z. Sheng, N. Falkner, X. Li, T. Gu, Tagfall: Towards unobstructive fine-grained fall detection based on uhf passive rfid tags, in: Proceedings of the 12th International Conference on Mobile and Ubiquitous Systems: Computing, Networking and Services, 2015, pp. 140–149.

[13] M. Breitenstein, F. Reichlin, B. Leibe, E. Koller-Meier, L. Van Gool, Online multiperson tracking-by-detection from a single, uncalibrated camera, IEEE Transactions on Pattern Analysis and Machine Intelligence 33 (9) (2011) 1820–1833.

[14] H. Dai, Z.-M. Zhu, X.-F. Gu, Multi-target indoor localization and tracking on video monitoring system in a wireless sensor network, Journal of Network and Computer Applications 36 (1) (2013) 228–234.

[15] B. Yang, Y. Lei, B. Yan, Distributed multi-human location algorithm using naive bayes classifier for a binary pyroelectric infrared sensor tracking system, IEEE Sensors Journal PP (99) (2015) 1–1.

[16] T. Helten, M. Muller, H.-P. Seidel, C. Theobalt, Real-time body tracking with one depth camera and inertial sensors, in: Proceedings of IEEE International Conference on Computer Vision (ICCV 2013), 2013, pp. 1105–1112.

[17] J. Wilson, N. Patwari, Radio tomographic imaging with wireless networks, IEEE Transactions on Mobile Computing 9 (5) (2010) 621–632.

[18] A. Saeed, A. Kosba, M. Youssef, Ichnaea: A low-overhead robust wlan device-free passive localization system, IEEE Journal of selected Topics in Signal Processing 8 (1) (2014) 5–15.

[19] K. Wu, J. Xiao, Y. Yi, D. Chen, X. Luo, L. Ni, Csi-based indoor localization, IEEE Transactions on Parallel and Distributed Systems 24 (7) (2013) 1300–1309.

[20] C. Wu, Z. Yang, Z. Zhou, X. Liu, Y. Liu, J. Cao, Non-invasive detection of moving and stationary human with wifi, IEEE Journal on Selected Areas in Communications 33 (11) (2015) 2329–2342.

[21] F. Adib, Z. Kabelac, D. Katabi, Multi-person localization via rf body reflections, in: Proceedings of the 12th USENIX Conference on Networked Systems Design and Implementation (NSDI 2015), 2015, pp. 279–292.

[22] J. Han, C. Qian, X. Wang, D. Ma, J. Zhao, W. Xi, Z. Jiang, Z. Wang, Twins: Device-free object tracking using passive tags, IEEE/ACM Transactions on Networking PP (99) (2015) 1–13.

[23] W. Ruan, L. Yao, Q. Z. Sheng, N. Falkner, X. Li, Device-free localization and tracking using passive rfid tags, in: Proceedings of the 11th International Conference on Mobile and Ubiquitous Systems: Computing, Networking and Services (MobiQuitous 2014), 2014, pp. 80–89.

[24] L. Yao, Q. Z. Sheng, W. Ruan, T. Gu, X. Li, N. Falkner, Z. Yang, Rfcare: Device-free posture recognition for elderly people using a passive rfid tag array, in: The international Conference on Mobile and Ubiquitous Systems: Computing, Networking and Services (MobiQuitous'15), 2015, pp. 120–129.

[25] W. Ruan, Unobtrusive human localization and activity recognition for supporting independent living of the elderly, in: Pervasive Computing and Communication Workshops (PerCom Workshops), 2016 IEEE International Conference on, IEEE, 2016, pp. 1–3.

[26] F. Rizzo, M. Barboni, L. Faggion, G. Azzalin, M. Sironi, Improved security for commercial container transports using an innovative active rfid system, Journal of Network and Computer Applications 34 (3) (2011) 846–852.

[27] L. A. Amaral, F. P. Hessel, E. A. Bezerra, J. C. Corrêa, O. B. Longhi, T. F. Dias, ecloudrfid–a mobile software framework architecture for pervasive rfid-based applications, Journal of Network and Computer Applications 34 (3) (2011) 972–979.

[28] D. M. Dobkin, The RF in RFID: UHF RFID in Practice, 2nd Edition, Newnes, 2012.

[29] L. Yang, Y. Guo, T. Liu, C. Wang, Y. Liu, Perceiving the slightest tag motion beyond localization, IEEE Transactions on Mobile Computing 14 (11) (2015) 2363–2375.

[30] C.-C. Chang, C.-J. Lin, LIBSVM: A library for support vector machines, ACM Transactions on Intelligent Systems and Technology 2 (2011) 27:1–27:27.

[31] C. Xu, B. Firner, Y. Zhang, R. Howard, J. Li, X. Lin, Improving rf-based device-free passive localization in cluttered indoor environments through probabilistic classification methods, in: Proceedings of the 11th International Conference on Information Processing in Sensor Networks (IPSN 2012), 2012, pp. 209–220.

[32] L. Kanaris, A. Kokkinis, G. Fortino, A. Liotta, S. Stavrou, Sample size determination algorithm for fingerprint-based indoor localization systems, Computer Networks 101 (2016) 169–177.

[33] L. Yao, W. Ruan, Q. Z. Sheng, X. Li, et al., Exploring tag-free rfid-based passive localization and tracking via learning-based probabilistic approaches, in: Proceedings of 23rd ACM International Conference on Information and Knowledge Management (CIKM 2014), 2014, pp. 1799–1802.

[34] P. Najera, J. Lopez, R. Roman, Real-time location and inpatient care systems based on passive rfid, Journal of Network and Computer Applications 34 (3) (2011) 980–989.

[35] M. Seifeldin, A. Saeed, A. E. Kosba, A. El-keyi, M. Youssef, Nuzzer: A large-scale device-free passive localization system for wireless environments, IEEE Transactions on Mobile Computing 12 (7) (2013) 1321–1334.

[36] X. Mao, S. Tang, J. Wang, X. Y. Li, ilight: Device-free passive tracking using wireless sensor networks, IEEE Sensors Journal 13 (10) (2013) 3785–3792.

[37] W. Li, J. Portilla, F. Moreno, G. Liang, T. Riesgo, Multiple feature points representation in target localization of wireless visual sensor networks, Journal of Network and Computer Applications 57 (2015) 119–128.

[38] D. Yuanfeng, Y. Dongkai, Y. Huilin, X. Chundi, Flexible indoor localization and tracking system based on mobile phone, Journal of Network and Computer Applications 69 (2016) 107–116.

[39] N. B. Priyantha, A. Chakraborty, H. Balakrishnan, The cricket location-support system, in: Proceedings of the 6th Annual International Conference on Mobile Computing and Networking (MobiCom 2000), 2000, pp. 32–43.

[40] B. Zhou, Q. Li, Q. Mao, W. Tu, X. Zhang, Activity sequence-based indoor pedestrian localization using smartphones, IEEE Transactions on Human-Machine Systems 45 (5) (2015) 562–574.

[41] H. Xie, T. Gu, X. Tao, H. Ye, J. Lu, A reliability-augmented particle filter for magnetic fingerprinting based indoor localization on smartphone, IEEE Transactions on Mobile Computing PP (99) (2015) 1–1.

[42] S. De Lausnay, L. De Strycker, J.-P. Goemaere, B. Nauwelaers, N. Stevens, A survey on multiple access visible light positioning, in: Emerging Technologies and Innovative Business Practices for the Trans-

formation of Societies (EmergiTech), IEEE International Conference on, IEEE, 2016, pp. 38–42.

[43] Y. Zhao, N. Patwari, J. M. Phillips, S. Venkatasubramanian, Radio tomographic imaging and tracking of stationary and moving people via kernel distance, in: Proceedings of the 12th International Conference on Information Processing in Sensor Networks (IPSN 2013), 2013, pp. 229–240.

[44] Y. Zhao, Y. Liu, T. He, A. Vasilakos, C. Hu, Fredi: Robust rss-based ranging with multipath effect and radio interference, in: Proceedings of the 32st IEEE International Conference on Computer Communications (INFOCOM 2013), 2013, pp. 505–509.

[45] A. Kokkinis, M. Raspopoulos, L. Kanaris, A. Liotta, S. Stavrou, Map-aided fingerprint-based indoor positioning, in: Personal Indoor and Mobile Radio Communications (PIMRC), 2013 IEEE 24th International Symposium on, IEEE, 2013, pp. 270–274.

[46] A. M. Hossain, W.-S. Soh, A survey of calibration-free indoor positioning systems, Computer Communications 66 (2015) 1–13.

[47] B. Wagner, N. Patwari, D. Timmermann, Passive rfid tomographic imaging for device-free user localization, in: Proceedings of the 9th Workshop on Positioning Navigation and Communication (WPNC 2012), 2012, pp. 120–125.
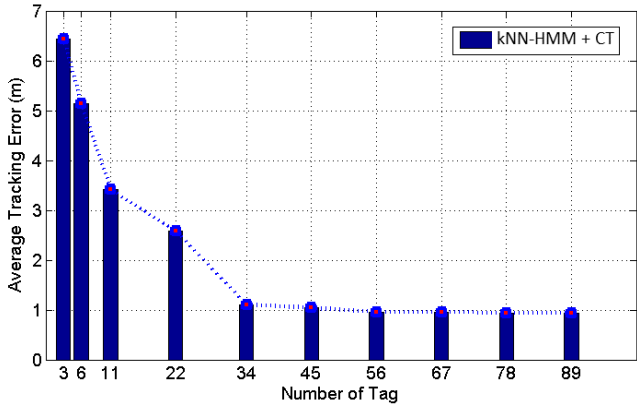
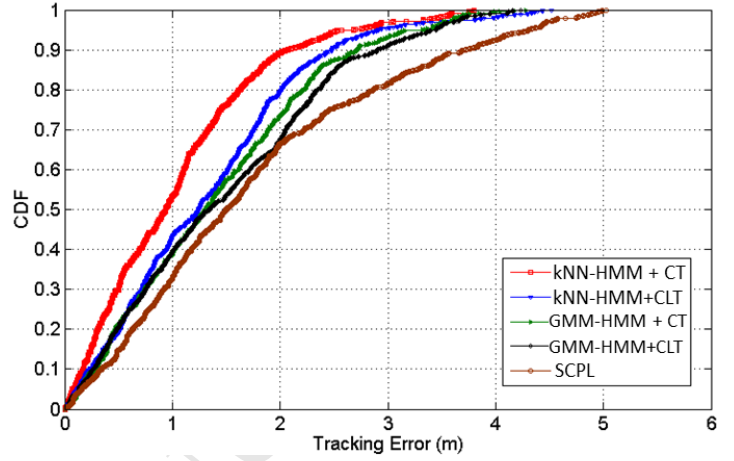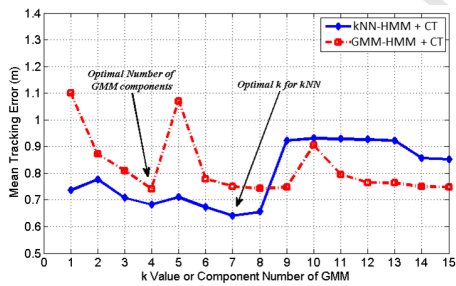Figure 26: Tracking errors with tag numbers

Figure 27: Tracking error CDF

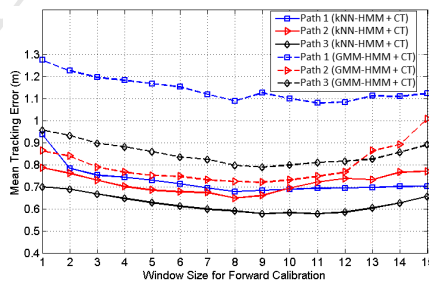Figure 28: k value and GMM component number
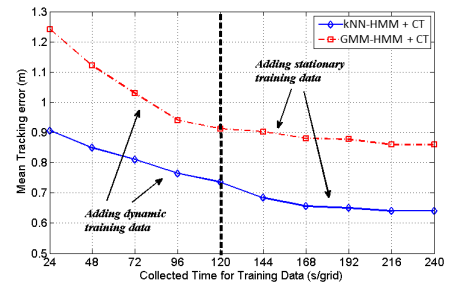

Figure 29: Window size in forward calibration

Figure 30: Stationary data vs dynamic data

Author Biography

Wenjie Ruan is a Postdoctoral Research Fellow in the Department of Computer Science, University of Oxford, UK. He obtained PhD at the School of Computer Science in the University of Adelaide, Australia. He received B.S. in Automation and MSc in Control Science and Engineering from Central South University, China, in 2010 and 2013 respectively. His research interests include the indoor localization and tracking, pervasive computing, and mobile computing. He has published close to 20 papers including CIKM, UbiComp, MobiQuitous, and PerCom. He has won a number of awards and prizes including SIGIR Travel Grant 2016, Best Poster Award at the 9th ACM Intl. Workshop on IoT and Cloud Computing, and Highly Commended Research Poster Award at the 25th Australia Database Conference (ADC 2014) PhD School.

Quan Z. Sheng received the PhD degree in computer science from the University of New South Wales, Sydney, Australia, in 2006. He is a full professor and head of Department of Computing, Macquarie University. His research interests include Web of Things, big data analytics, distributed computing, Internet technologies, and sensor networks. He received the ARC Future Fellowship, in 2014, Chris Wallace Award for Outstanding Research Contribution, in 2012, Microsoft Research Fellowship, in 2003, and CSC Fellowship, in 1998. He has more than 270 publications and is a member of the IEEE and the ACM.

Lina Yao is currently a lecturer at School of Computer Science and Engineering, the University of New South Wales (UNSW Australia). She received her PhD degree in Computer Science from the University of Adelaide in 2014. Her research interests include Internet/Web of Things analytics, Web mining, service computing and ubiquitous and pervasive computing. She is awarded an ARC (Australian Research Council) Discovery Early Career Researcher Award (DECRA) in 2015. She is the author of more than 50 publications. She is a member of the ACM and IEEE.

Xue Li received the MS and PhD degrees from The University of Queensland and the Queensland University of Technology in 1990 and 1997, respectively. Currently, he is a full professor in the School of Information Technology and Electrical Engineering, The University of Queensland in Brisbane, Queensland, Australia. His major areas of research interests and expertise include: data mining, multimedia data security, database systems, and intelligent web information systems. He is a member of the ACM, the IEEE, and SIGKDD.

Nickolas J.G. Falkner is an Associate Professor in the School of Computer Science at the University of Adelaide. He conducts research into computer network design and development, network security, privacy preservation, the Internet of Things and educational research, with a focus on increasing student participation, retention, and enthusiasm. Recently, he has begun working in the area of Smart Cities, as part of unifying his network and IoT research within one theme.

Lei Yang is the Research Assistant Professor in Department of Computing, Hong Kong Polytechnic University. Previously, he was a postdoc fellow in the School of Software, Tsinghua University. He received his B.S. and Ph.D degree from the School of Software and the department of Computer Science and Technology respectively, from Xi'an Jiaotong University. He is the winner of the Best Paper Award at MobiCom'14 and MobiHoc'14, a Runner-up of Best Video Award at MobiCom'16. He is also the recipient of ACM China Doctoral Dissertation Award. His research interests include RFID, backscatter and wireless communication, mobile computing.